



Contents lists available at ScienceDirect

Arabian Journal of Chemistry

journal homepage: www.ksu.edu.sa

Original article

Differences between two plants fruits: *Amomum tsaoko* and *Amomum maximum*, using the SPME-GC–MS and FT-NIR to classificationFengjiao Li^{a,b}, Weize Yang^a, Meiquan Yang^a, Yuanzhong Wang^{a,*}, Jinyu Zhang^{a,*}^a Medicinal Plants Research Institute, Yunnan Academy of Agricultural Sciences, Kunming 650223, China^b School of Agriculture, Yunnan University, Kunming 650223, China

ARTICLE INFO

Keywords:

Amomum tsaoko Crevost et Lemaire*Amomum maximum* Roxb.

GC–MS

FT-NIR

Classification

ABSTRACT

Also known as *Amomum tsaoko* Crevost et Lemaire (*A. tsaoko*), is a spice and medicinal fruit plant that can be used in daily human life for cooking and health purposes. In Xishuangbanna (Yunnan Province, China) there is an interesting phenomenon where the *Amomum maximum* Roxb. (*A. maximum*) is consumed as a fruit by the local people. The spice trade played a significant role in the development of human civilization and the histories of nations. Both of them have high edible and medicinal value. The identification and classification of the metabolic components of both are key to driving the development of related industries. We used SPME-GC–MS (Non-targeted headspace-solid phase microextraction-gas chromatography-mass spectrometry) for its accurate qualitative and quantitative performance, combined with multiple analytical methods, to explain the metabolic components present in the fruits of these two plants. Next, near-infrared (NIR) technology offers researchers the advantage of saving time and being cost-effective. We analyzed the characteristic spectral chemical information of the NIR data. Identified the relevant base group and vibration mode. After analyzing the data of both, it was determined that there are a total of 66 metabolites, with 64 from cardamom and 29 from the substance, showing 37 differences. Among the metabolites, 35 had a significance level of $P \leq 0.05$ and $VIP \geq 1$, totaling 101 substances. This includes terpenes (37.9 %), aldehydes (12.1 %), organic heterocyclic compounds (7.6 %), alcohols (6.1 %), aromatic compounds (4.5 %), esters (4.5 %), and ketones (4.5 %). This study validates the metabolic components of the two species and provides a clear classification, which will be beneficial for future data-based applications in the fields of food and medicine.

1. Introduction

For over 600 years, it has been planted and distributed along the border in China. It is a traditional Chinese spice with versatile functions in food and medicine, and it is a perennial tufted herb. In traditional oriental medicine, the dried fruit of *A. tsaoko* has been used to treat malaria, throat infections, abdominal pain, stomach disorders, dyspepsia, nausea, vomiting, and diarrhea (Huiwei et al., 2021). Usually used as a seasoning in meat dishes, hotpot, and various soups to eliminate any unpleasant odors (Lim, 2013, Wang et al., 2021). It has been approved to be included in the list of homologous drugs and foods in China (Liang et al., 2023). Its flavor is characterized by a pungent and spicy taste, accompanied by a distinctive aroma. The essential oil demonstrates a broad spectrum of physiological activities, encompassing antibacterial, antioxidant (Fan et al., 2023), and anti-tumor properties (Cui et al., 2017) etc. However, the current focus of metabolic

component research is primarily on the extraction of volatile oil from dried fruits. Bioactive ingredients are often reported as phenols, flavonoids, terpenoids, and so on (He et al., 2020, Shi et al., 2021).

A. maximum is often eaten as a fruit in Xishuangbanna, sweet and slightly sour by the fresh fruit period (Huang, 2017). Currently, it is mainly produced in southern Tibet, Yunnan, Guangdong, and Guangxi Province, and it is distributed from South Asia to Southeast Asia. It possesses traditional therapeutic potential and culinary effects. The forest habitat is generally shady and humid, typically at altitudes ranging from 350 to 800 m. The flowering period is from May to June, and the fruiting period is from June to August. When the fruit is used for medicinal purposes, it can act as an appetizer, aid digestion, regulate qi, and relieve pain (Kuang et al., 2020). The isolation of labdane diterpenes from the rhizomes of this species, which have demonstrated anti-hyperglycemic properties, is of particular interest. This finding suggests a potential beneficial role in diabetes management (Lu et al., 2021).

* Corresponding authors.

E-mail addresses: boletus@126.com (Y. Wang), jy Zhang@126.com (J. Zhang).<https://doi.org/10.1016/j.arabjc.2024.105665>

Received 28 October 2023; Accepted 3 February 2024

Available online 10 February 2024

1878-5352/© 2024 The Author(s). Published by Elsevier B.V. on behalf of King Saud University. This is an open access article under the CC BY-NC-ND license (<http://creativecommons.org/licenses/by-nc-nd/4.0/>).

According to existing reports, the components extracted from different parts of this species' plants exhibit rich biological activity. (Lu et al., 2021). The content mainly revolves around cytotoxicity (Luo et al., 2014), anti-inflammatory activity (Ji et al., 2018), and insecticidal activity (Guo et al., 2015). The two species are shown in Fig. 1.

Nevertheless, after drying, the appearance of the fruit seems to be similar, with the surface of both fruits predominantly brown in color. If a large quantity of two kinds of fruits are mixed in the same market sack, the consumer cannot distinguish them simply by natural senses and may mistakenly think that they are the same kind of plant fruit. As a result, the use of the raw material does not bring out the social and economic value of its metabolic components in terms of edible and medicinal uses.

The traditional methods of identifying the species and quality usually include the fruit's shape, color, size, and scent, all based on subjective judgment. GC-MS can be used as an analysis technology for differentiating species, processing, and growth years, which is a reliable tool.

Metabolites are the intermediates of metabolic reactions that take place in cells. Metabolomics is an emerging science, which can detect the existence of hundreds of metabolites, is widely used in the study of plant metabolites, screening of biomarkers, dual-use of medicine and food, breeding of effective ingredients and qualitative varieties, etc (Hew et al., 2024). Various short-chain alcohols, aldehydes, ketones, esters, aromatic phenols and lactones, as well as monoterpenes and

sesquiterpenes are often volatile chemicals produced by plants (Leather, 2009). For herbivorous insects, the quality of the host plant and its species differences can affect the insect's growth, survival, quality, and immune function (Karlsson Green, 2021). Laboratory investigations have found that 1 ~ 50 mg/mL, the crude extract of cardamom, can cause the disintegration of parasites in phosphate-buffered salt water, a natural pesticide (Chetia et al., 2014). Therefore, the study of two plants from the perspective of plant pest control can provide a reference for the prediction and integrated management of pests. Correspondingly, this research is also significant and exciting.

Because the qualitative analysis of GC-MS can not only rely on the mass spectrum library, the separation effect is closely related to the reliability of the retrieval matching rate. The chromatography retention time and a series of information related to samples are essential for qualitative analysis. The advantage of GC-MS is that the same sample has different separation conditions. Hundreds of components may be identified, or only dozens of individual components may be identified. However, under the premise of correct MS spectra, the specificity of MS is recognized. Since the 1990 s, SPME has been considered a simple, efficient, and environmentally friendly sample preparation technique (Arthur and Pawliszyn, 1990). From an environmental perspective, especially when compared to traditional sample preparation methods, SPME is very attractive. It requires almost no organic solvents or other

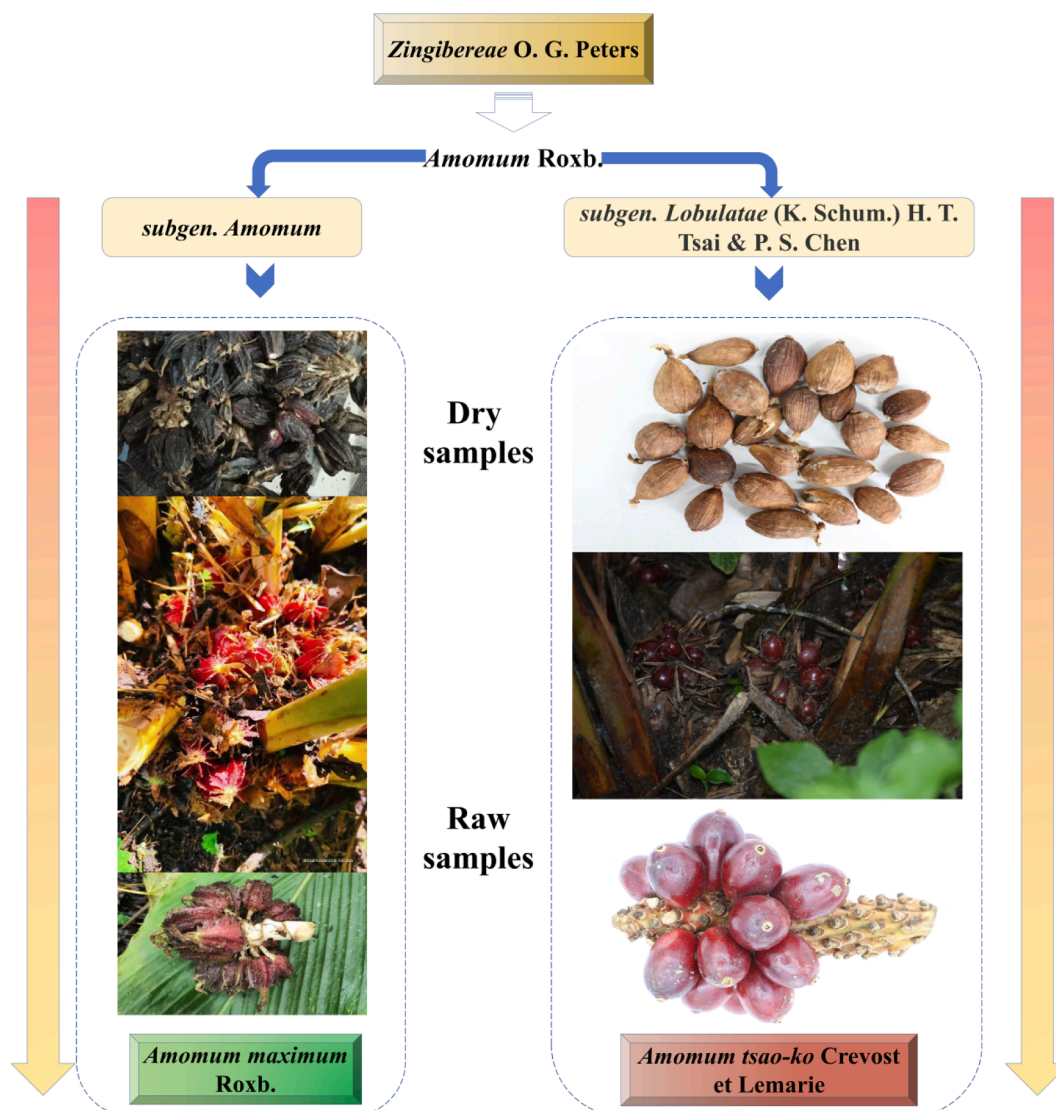


Fig. 1. The plant parts of *Amomum tsao-ko* Crevost et Lemarie (Right) and *Amomum maximum* Roxb.(Left).

sample preparation steps and produces very little chemical waste. SPME aim to extract analytes in proportion to their free concentrations in the sample for analysis (Zhou et al., 2023). NIR can carry a lot of chemical information and has the advantage of fast-saving sample materials. The statistical analysis of the NIR series enables the rapid identification of two species to provide certain scientific references in necessary and specific detection scenarios. Excellent interpretation can be produced, and the information can be complementary with GC-MS to achieve the common identification of grass fruit and cardamom. Since this time, an immense amount of new information has become available, and presenting all this information in such a compact and accessible manner is a meaningful study. However, GC-MS is subject to different conditions for the detection of metabolites. The differential metabolites detected are not the same. Therefore, the current metabolomics of *A. tsaoko* and *A. maximum* is only based on the identifying of simple metabolites. On this basis, it is necessary to conduct an in-depth exploration of metabolites, to explore the mechanism of metabolism, and to understand the fruit components of the two species transparently. Further analysis and analysis are needed, and this research also lays a strong foundation for further research a perfect foundation.

In conclusion, this study aims to utilize modern technology to ultimately achieve the classification of different metabolic components in two species. Our proposal provides new evidence of the two fruits' DAM (Differential metabolite analysis) composition and relative content. It also verified the feasibility of NIR technology to identify the above two fruits and the performance of the classical model.

2. Materials and methods

2.1. Plant materials prepare

The dried plant products purchased after visiting the market research (Purchase date: October 2021), *A. tsaoko* was obtained in Guangxi Provinces (China). The study team collected *A. maximum* in the Planting base. The samples were identified as the fruits of *Amomum tsaoko* Crevoet et Lemarie (D) and *Amomum maximum* Roxb. (F) of *Zingiberaceae* by Dr. Jinyu Zhang (Medicinal Plants Research Institute, Yunnan Academy of Agricultural Sciences, Kunming, China). Prepared: First, we took dried fruits D and F, cracked them with a small hammer. Subsequently, they were placed in an agate mortar, into which liquid nitrogen was added for grinding until the grinding solution achieved a complete and uniform mixture.

GC-MS: The collected samples were divided into three parts, three biological repeats were repeated, and three parallel experiments were carried out to eliminate the batch effect and comply with the basic rules of statistics.

2.2. GC-MS detection

2.2.1. Solid-phase microextraction (SPME)

The SPME of information: Equipment: CTC Trinity Autosampler; Extraction: 50/30 $\mu\text{mDVB/CARonPDMS}$; Temperature: 50°C; Time: shock 15 min, extraction: 30 min, Concussion speed: 250 rpm; Parsing time: 5 min; GC cycle time: 50 min.

2.2.2. Operating conditions

Used DB-wax (30 m \times 0.25 mm \times 0.25 μm), the derivative substances were separated by constant flow helium of 1 mL/min, 0.5 g sample was added to the 20 mL headspace bottle and sealed. The temperature of the injection port is 260°C, the initial temperature is 40°C, the 5 min is maintained, the temperature rises to 220°C at the rate of 5°C/min, and the temperature rises to 250°C at the rate of 20°C/min, keeping 2.5 min. Interface temperature: 260 °C; Ion source temperature: 230 °C; Four-stage rod temperature: 150 °C; Ionization mode: EI+, 70 eV; Scanning method: full scan; Mass range: 20 ~ 400. The instrument GC-MS shown in Table 1. NIST2014 of spectral library. All metabolites

Table 1

Metabolomics detection instrument GC-MS.

Name	Brand	Model
Gas Chromatograph	Agilent	7890B
Mass spectrometer	LECO	Pegasus BT

were obtained from the following databases: Panomic's own standard database (Suzhou, China) and the PubChem data (PubChem (nih.gov)).

2.2.3. Data optimization

Firstly, obtain the names of possible metabolites in each sample and their retention time, CAS number, related content, and other information through database annotation and integrate that annotation information of each sample to obtain the final table of possible metabolites for analysis. Secondly, to enable the data of different magnitudes to be compared, the standard internal normalization of the peak area is performed on the data. Internal standard: Benzene, 1,4-dichloro-, 100 $\mu\text{g}/\text{mL} \times 10 \mu\text{L}$, which is convert the relative content of each component.

2.3. NIR data for obtain

The Antaris II Fourier Transform Near Infrared Spectroscopy (Thermo Fisher Scientific INC., USA) was used for measuring the fruits of D and F powder. The two kinds of dried fruits collected were crushed by a pulverizer, screened for 100 mesh, sealed in a sealed bag, and placed in a cool and dry place. The wavelength range from 10,000 to 4000 cm^{-1} was set 32 times, a total of 3 repetitions, and finally, the average spectrum was obtained for data analysis. The laboratory conditions are required to temperature is 25 °C, and air humidity is 45 %. For the clear study achievement display, Origin Lab 2022b software was utilized for the draw average NIR and featured variable spectra.

2.4. Statistical analysis

Metabolomics data and spectral data are both complex data languages, each containing multidimensional and correlated information. Traditionally, univariate analysis cannot quickly, thoroughly, and accurately mine potential information in the data. Therefore, multivariate statistical methods are proposed for the imputation and qualitative analysis of the collected multidimensional data. Preliminary results were obtained by automatic scaling, Mean-centering, and scaling to unit variance (UV) of the raw data before multivariate statistical analysis.

2.4.1. Overall metabolite hierarchical clustering analysis

Conduct cluster analysis on the metabolite data to explore differences between the two species. Cluster heat maps showing the correlation of the data were drawn using R software. The heat map is the quality control of experimental data and the display of differential data. A single heat map is composed of a heat map body and heat map components. In the study, we adapt that agglomerate hierarchical clustering: Group each object into one class and merge these classes into larger and larger objects until the end. The data set is then scaled using the heatmap package in R (v3.3.2) and the relative quantitative values of the metabolites. Hierarchical clustering analysis is suitable for evaluating the similarity between samples. The distance calculation method, Euclidean clustering, calculates the pairwise distance between the respective data points of the two categories (Yuan et al., 2012).

2.4.2. Statistical analysis of differential metabolites

A Venn diagram is a graphical representation showing the overlapping areas of elements. It visually represents the similarity and overlap of different metabolite compositions in various comparison sets.

The box plots: A box plot is a statistical chart used to display the dispersion of a set of data, providing a relatively intuitive way to

visualize the data distribution characteristics. Each data group can present its minimum, maximum, and average, and the range between the minimum and maximum values reflect the degree of variation in the data. Bar chart: The bar chart is a statistical report chart that uses the length of a rectangle as the variable for the graphical representation. It consists of a series of vertical bars of varying heights that indicate the distribution of the data, along with error lines indicating the standard error.

2.4.3. Multivariate statistical analysis

PCA generates new characteristic variables by linearly combining metabolite/spectrum variables with certain weights, categorizing each data group by the primary new variable (principal component). On top

of that, it also removes poorly reproducible samples (outlier samples) and abnormal samples (samples outside the confidence interval, Hotelling T^2 ellipse). The reliability of the mathematical model calculated by PCA needs to be rigorously validated. An unreliable mathematical model fails to characterize the metabolomics data well and may seriously affect the acquisition of correct results or even mislead the analysis results. Therefore, the constructed model needs to be validated. The cross-validation of models mainly refers to parameters such as R^2X , which is the interpretability degree of the model. Usually, R^2 higher than 0.5 is better.

The unsupervised analysis method must recognize intra-group errors, eliminate random errors unrelated to the study's purpose, avoid excessive focus on details at the expense of overall patterns, and

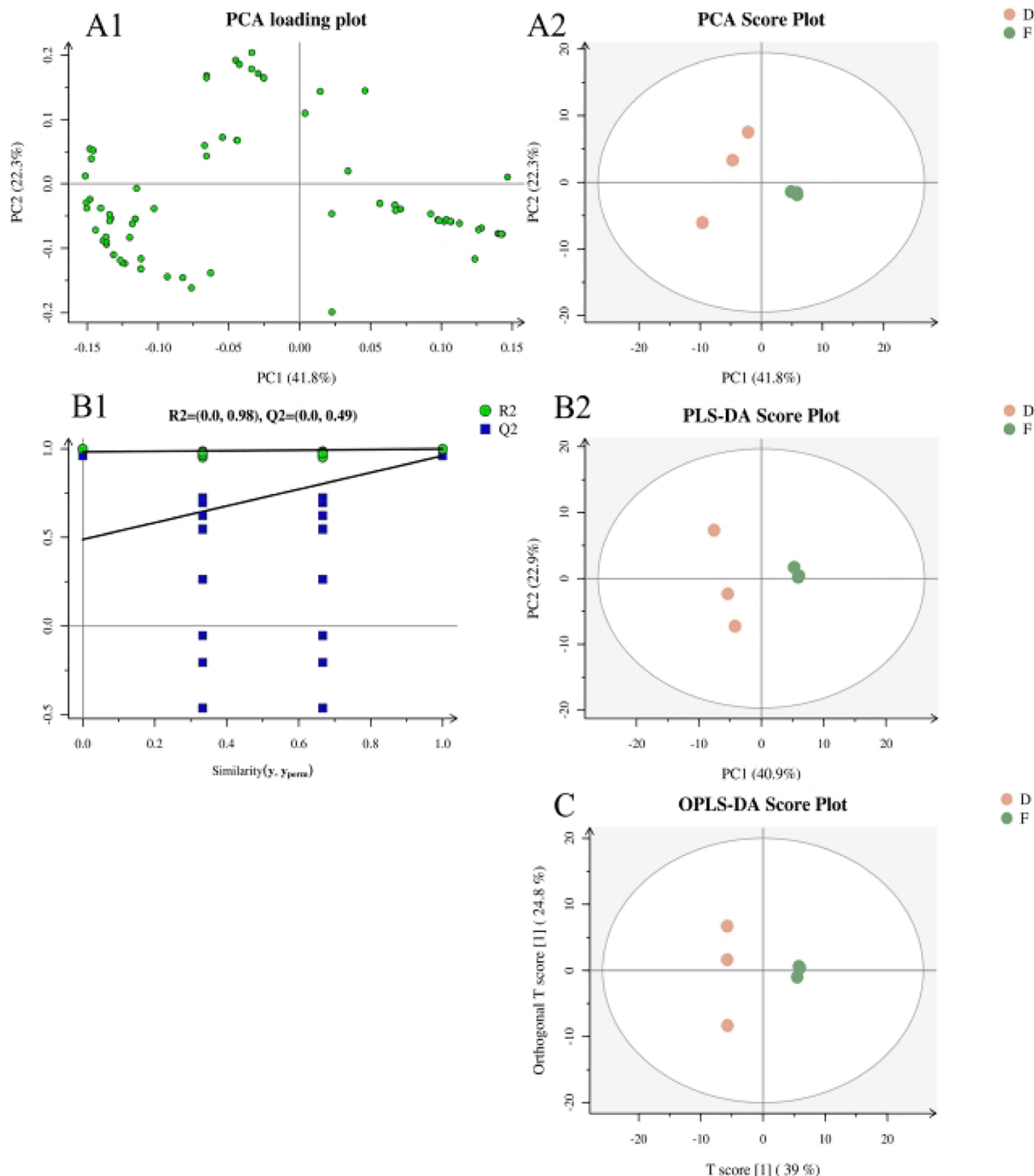


Fig. 2. GC-MS of the PCA and PLS-DA model. (A1: PCA loading plot; A2: PCA Score Plot; B1: permutation test; B2: PLS-DA Score Plot; C: OPLS-DA).

ultimately facilitate the discovery of inter-group differences and differential compounds. Therefore, this study sticks to this point, thus proposing using PLS-DA for analysis. PLS-DA commonly used pattern multivariate statistical analysis tool, which was a match for dealing with highly correlated variables. It combines the regression model with dimensionality reduction and utilizes specific discriminant thresholds to analyze the regression results. Compared with PLS-DA, OPLS can effectively reduce the model's complexity and enhance the model's explanatory power without reducing the model's predictive power, thus maximizing the variance of the formation. (Document of SIMCA-P 13.0) R^2 is the goodness of fit, which is the percentage of the variation between the training set Y explained by the model and the partial least squares. as the degree of fit of the model to the data. Close to the value of 1 to the R^2 is a necessary condition for the existence of an excellent model. Q^2 is the prediction superiority as the percentage of variance between the cross-validated prediction training set X and the partial least squares. Q^2 indicates the degree to which the new data are predicted, and larger values, indicate that the model has good prediction performance.

2.5. Software

Metabolic data were mainly obtained using R software (<https://www.r-project.org/>), Spectroscopy data were utilized OMNIC (The data processing software that comes with the instrument), SIMCA P + 14.1 (Umetrics, Sweden, www.sartorius.com), and the OriginPro 2022 (<https://www.originlab.com/>) take the initiative to plot multivariate statistical analysis.

3. Results and discussion

3.1. The GC-MS of the results

3.1.1. Multivariate statistical analysis

A total of 101 kinds of metabolites in D and F were detected, shown in **Table S1**. The differences between species are visualized from the PCA plot, and it is clear that D and F have been separated, but for F, its poor clustering effect is shown in **Fig. 2 A**. Data dimensionality is reduced for visual sample analysis. The metabolite PCA score shows that the two principal components have successfully explained 64.1 % of the information with an R^2X (cum) value of 0.641 and a pre of 2. The biological repeat distribution of F is closer than that of D, indicating that the intraspecific variation of F is relatively tiny. Moreover, the distribution of D is also different from that of F, thus indicating the validity of the model, technical variability, and lower level of biological variation.

HCA of the GC-MS data revealed that the six samples clustered into two major groups (**Fig. S1**), indicating differences in metabolites among the samples. The HCA diagram shows that D and F were strictly divided into two main components. This result is consistent with the PCA, where F acquired by growers could cluster together. At the same time, there was a clear difference between the D samples purchased through the market.

We can tell from the final results that D compounds were divided into 17 classes (the following only lists categories more remarkable than 3 %), including the terpenes (37.9 %), aldehydes (12.1 %), organic heterocyclic compounds (7.6 %), alcohols (6.1 %), aromatic (4.5 %), esters (4.5 %), ketones (4.5 %), peptide (3 %) being the predominant metabolite classes. On the contrary, F is divided into a total of 17 categories, of which, as the main metabolic categories, are terpenes (37.5 %), esters (12.5 %), alcohols (9.4 %), aldehydes (6.3 %), alkanes (7.8 %), aromatic (3.1 %), carboxylic acid (3.1 %), olefin (3.1 %). A more specific visualization of the classification information is shown in **Fig. 3**.

Finally, a total of 101 metabolites were detected. The cluster analysis was used to determine the expression of metabolite relevance under different conditions or bases of metabolite visualization. A hierarchical clustering diagram of relative quantitative values of metabolites will be

obtained, as shown in **Fig. 4**. The magnitude of relative content in the graph is shown by the difference in color, where the columns represent samples and the rows represent metabolites. The above results indicate that the composition of metabolite classes was approximately the same between the studied D and F species.

Subsequently, using the HCA to reveals the magnitude of similarity between samples. Metabolite distribution and production are usually due to plant growth environment, growth stage, internal gene regulation, plant site differences, etc. According to the results obtained in this test, the amounts of D and F are also relatively close for terpenoids. D contains abundance of aldehydes more than F. For aromatic, this class of metabolites, as the aromatic odor of plants, has more D than F. The results of the comparison of the above two detected metabolite components are shown in the Venn diagram (Software: OriginPro 2022, ChemBioDraw Ultra 14.0, **Figure S2**). There are 29 metabolites in common; D and F have 37 and 35 different metabolites, respectively. Please refer to **Figure S5-S7** and **Table S5** for the specific chemical structures.

Histograms of two species show multiple metabolic species' relative content (**Figure S3**). Among the first five metabolites detected, the D fruit contained the following substances: Limonene, *-Terpineol, *-Muuroleone, Copaene, 2-Decenal, (Z)-. F included Bicyclo[3.1.1]heptane, 6,6-dimethyl-2-methylene-, (1S)-, Naphthalene, decahydro-4a-methyl-1-methylene-7-(1-methylethenyl)-, [4aR-(4a*,7*,8a*)]-, 1,3,7-Octatriene, 3,7-dimethyl-, Humulene, (-)-*-Bourbonene exhibited a higher relative content. These substances were inconsistent in each of the replicate samples, indicating a large genetic diversity in the two species.

The fruit of D, its unique flavor is associated with the composition of aromatic, stimulating compounds, most of which are monoterpenes, of which TPS is the critical enzyme involved in the biosynthesis of D. The researcher attempts to elucidate who utilized the crude enzyme extract of *A. tsaoko* combined with geraniol would have stimulatory expression (Ping Li et al., 2022). The metabolites of aromatics include Estragole, p-Xylene, Toluene and Creosol.

The **Fig. 2 B** reveal the total explanatory power is 63.8 %. Furthermore, it is worth mentioning that PLS-DA can extract the variation information between groups more efficiently and maximize the separation of assigned groups.

Finally, the metabolite with a VIP value greater than 1 under the OPLS-DA condition was selected as the difference value. OPLS-DA can decompose the X matrix information into two types of information related to Y and irrelevant. Then, after filtering out the information irrelevant to the classification, the relevant information mainly concentrated in the first prediction component, and the principal component 1 of this test was 39 %. **Table 2** indicates the specific model parameters of GC-MS.

Conditions of differential metabolite screening: The differential metabolite biomarker was searched for by screening metabolites, and the conditions of relevant metabolite screening were $p\text{-value} \leq 0.05 + \text{VIP} \geq 1$ (Trygg and Wold, 2002, Haspel et al., 2014, Wang et al., 2014, Kieffer et al., 2016).

3.1.2. Discussion: The metabolites in the samples of analysis

The aromatic and pungent odor of D is associated with its rich terpene content. The metabolites of the two species that contain the most classes are terpenes. Terpenoids are a general term for a class of hydrocarbons with the molecular formula of isoprene integer ($(C_5H_8)_n$), which are widely found in plants and marine organisms. These molecules can also undergo oxidation, rearrangement, and other chemical structural modifications to produce various alcohols, aldehydes, ketones, carboxylic acids, esters, and other terpenoid structures collective referred to as terpenes in a broad sense. Terpenoids (Boysen and Hearn, 2010) are the main natural products of many plant essential oils. They are used in large quantities in the food industry, cosmetics and even drugs. Such as limonene ($C_{10}H_{16}$), a monoterpene molecule with lemon

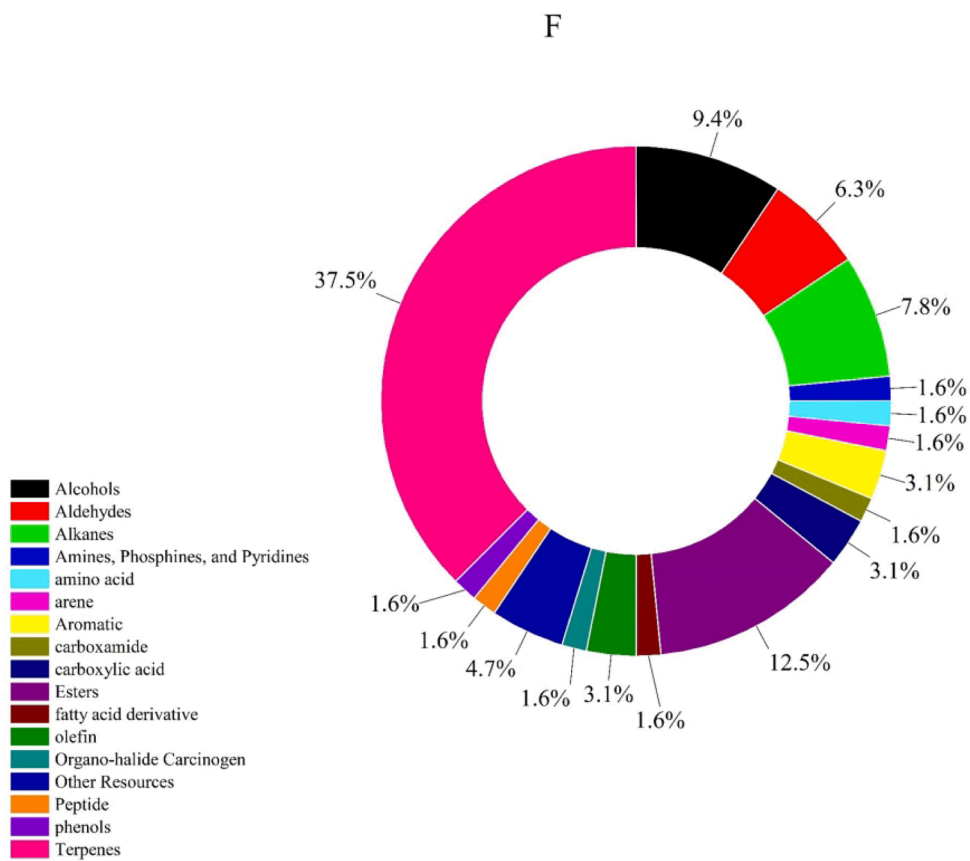
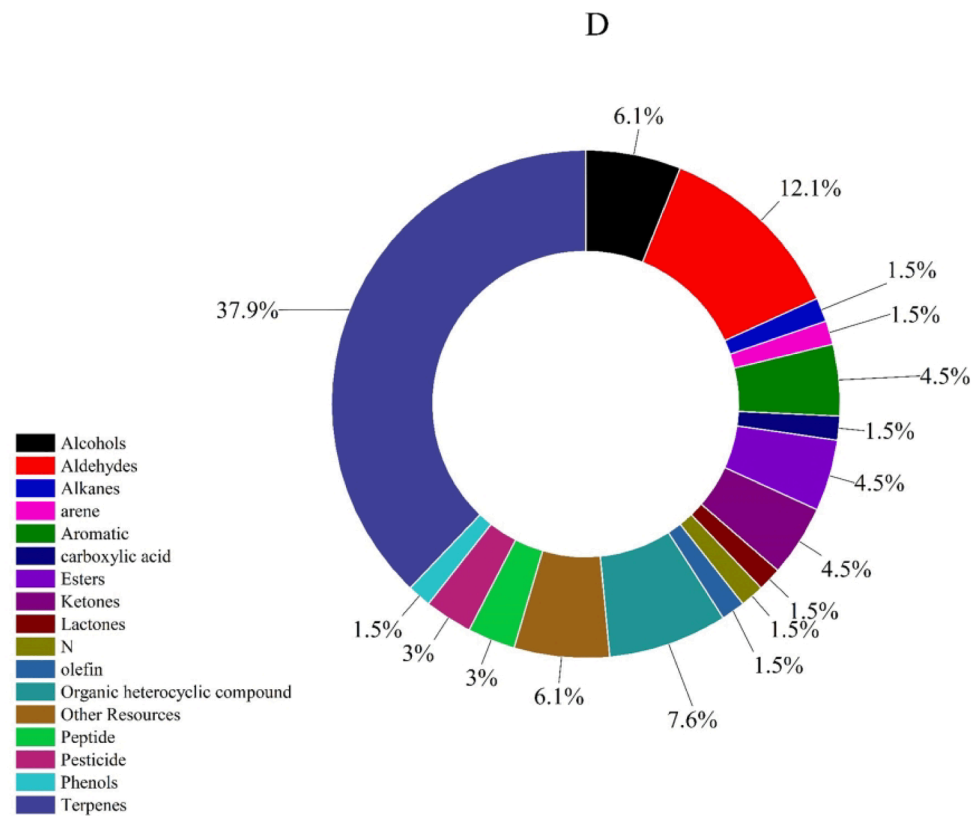


Fig. 3. GC-MS of the D and F comparison of various metabolite. D: *Amomum tsaoko* Crevost et Lemarie; F: *Amomum maximum* Roxb.).

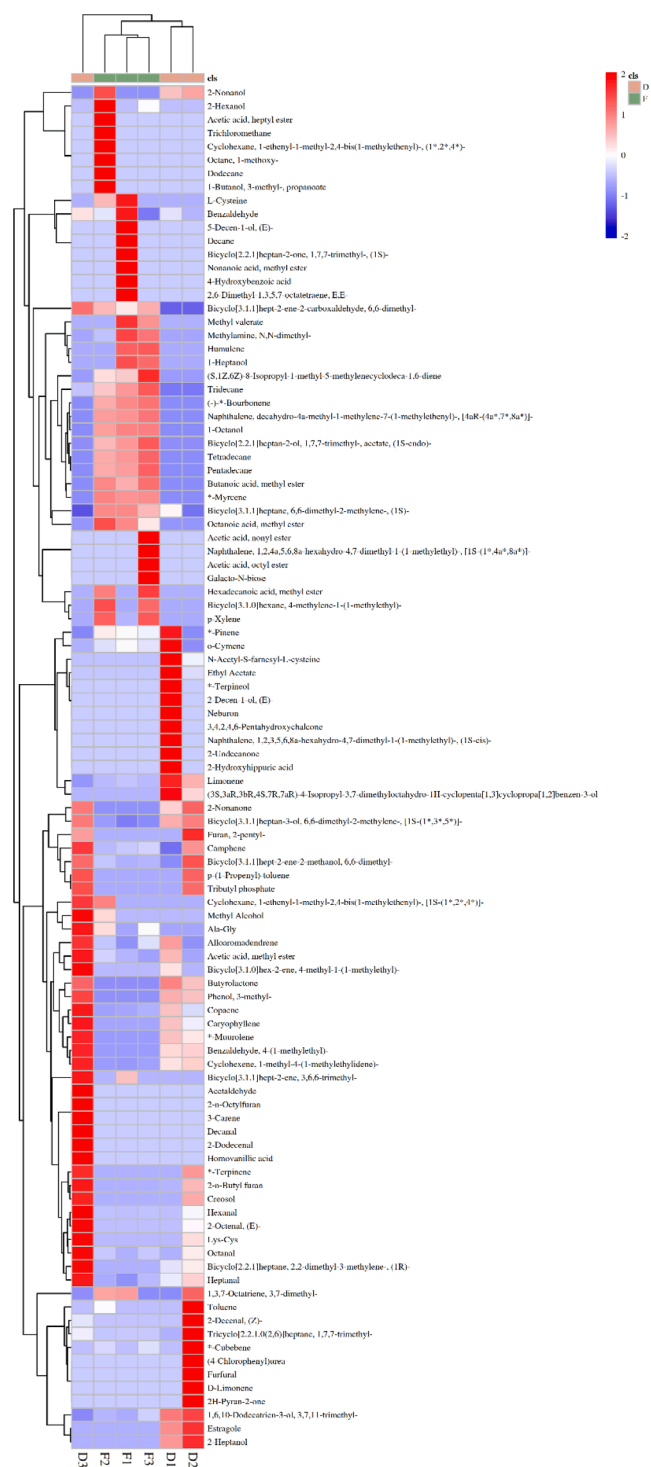


Fig. 4. The clustering heat map of metabolites of two species. D1, D2, D3: *Amomum tsaoko* Crevost et Lemarie; F1, F2, F3: *Amomum maximum* Roxb.).

Table 2

Model parameters of GC–MS for D vs F.

Model	pre	R2X(cum)	R2Y(cum)	Q2(cum)
PCA	2	0.641		
PLS-DA	2	0.638	0.999	0.96
OPLS-DA	1 + 1 + 0	0.638	0.999	0.855

aroma, or paclitaxel, a tricyclic diterpene with anticancer activity. Terpene synthase (TPS) has been found to be in terpenoid synthesis. The precursors were converted to monoterpenes, sesquiterpenes, and diterpenes, respectively (Wang et al., 2018a; Wang et al., 2018b). Terpenes are rightfully considered one of the largest classes of plant primary metabolites. Such metabolites can protect plants from environmental stress, surprisingly, have defenses against pathogens and herbivores (Wagner and Elmadfa, 2003, Huang et al., 2010, Goyal et al., 2012). The chiral identification of monoterpenes is crucial in the fields of spice chemistry and pharmacology (Boysen and Hearn, 2010). Monoterpenes and sesquiterpenes are the main components of volatile oils. Diterpenes are the main substances for forming resins; triterpenes are important substances for forming plant saponins and resins; tetraterpenes are mainly some fat-soluble pigments widely distributed in plants. Some of them have physiological activities, such as roundworm repellent, santonin with roundworm repellent effect, artemisinin with antimalarial effect, and andrographolide with antibacterial effect. Monoterpenes are synthesized in the plastids via the DOXP pathway; fatty acid derivatives are mainly produced by intermediates of the lipoxygenase-peroxidase pathway (Verdonk et al., 2003). Sesquiterpenes are often associated with mechanisms of organism protection. For instance, in marine green algae, in marine green algae, they are stored as polyacetates products and released as deterrent sesquiterpenes upon injury (Boysen and Hearn, 2010). The plant hormone abscisic acid is a sesquiterpene that induces fruit ripening and defoliation. Diterpenes can inhibit cell division and use in anticancer. Plant-derived diterpenes products have gibberellins and phytoalexins (defense) (Boysen and Hearn, 2010). This report shows a greater concentration on monoterpenes and sesquiterpenes for D and F. Sesquiterpenoids associated with spicy taste, Caryophyllene (Feng et al., 2017). Based on relevant evidence, isoprene, and β -caryophyllene have ecological functions as core components of plant signaling networks (Frank et al., 2021). Both have allelopathic chemical components that induce resistance to microbial pathogens in neighboring plants. This knowledge can be used to enhance plant resistance in various crop management programs, providing theoretical support.

Other reports that by GC–MS, were identified 73 compounds, including that monoterpenoids, sesquiterpenoids, diterpenoids, triterpenoids, diarylheptanoids, flavones, phenolic, etc. The main compositions were 1,8-cineole, ρ -propylbenzaldehyde, geraniol, geranial, α -terpineol, α -phellandrene (Yang et al., 2008) and fatty acid (Hang Liu et al., 2018).

Their aromatic and pungent properties are attributed to volatile and non-volatile, respectively (Starkenmann et al., 2007). It has been shown that there is a positive correlation between altitude and the yield of metabolites in D fruits, especially the aromatic components of the fruits, including 1,8-cineole, *trans*-citral, and the pungent compound, the decreasing trend at high altitudes of > 2000 m (Ping Li et al., 2022). An investigation was carried out to assess the presence of monoterpene hydrocarbons, oxygenated monoterpenes, sesquiterpene hydrocarbons, oxygenated sesquiterpenes, and other compounds in the fruits of D. Generally speaking, 1,8-Cineole is a kind of the oxygenated monoterpene, the main aroma component, with camphor, a cool and spicy flavor, as the most important constituent in oils (45.24 %) (Yang et al., 2010, Cui et al., 2017, Na Guo et al., 2017). Easily affected by light, temperature (Yi Lin et al., 2022), etc. However, the results of the current study did not find a clear explanation. This could be due to the prolonged storage time of the samples, the mixed storage of previous years by the vendors, the low content of growth and metabolism, or the differences in the methods of detection instruments. Then, there are no reports on the effects of storage periods of *A. tsaoko* on the quality of its processed products. Therefore, the storage period of *A. tsaoko* will become a hot research topic in the following period. Compounds will be decomposed and transformed under certain conditions. For example, limonene and linalool can be transformed into α -terpineol under certain conditions (Haleva-Toledo et al., 1999). D volatiles component has sedative, analgesic and hypnotic effects. The fruits of the 1,8 -Cineole

make up 45.2 % (Sabulal and Baby, 2021). Studies have confirmed that the strong spice smell released by the crushed fruit is mainly related to 1,8-Cineole, α -phellandrene, α -pinene, β -pinene, and 2-isopropylbenzaldehyde (Zhangguo Lu et al., 2010). As a result, Pinene, as a typical terpene, is present in D and F. Caryophyllene has three isomers α , β , and γ . β -Caryophyllene is a bicyclic sesquiterpene also common in spices that is a ligand of the cannabinoid receptor 2 (CB2), which can decrease pain for inflammatory responses and enhances wound healing (Koyama et al., 2019). Moreover, the above metabolites are only found in D. This exploratory study, for the first time, found Neburon, but it's only found in D1, only skeptical about such compounds. Since it is impossible to test the sample grass fruit again directly, there is only one guess: It is likely that the growers used it to remove weeds, and the residues were absorbed from the soil during the growth and development of plants (JR. et al., 1981).

Aromatic compounds have excellent stability, which is related to their fully conjugated monocyclic compounds structure with a planar geometry. According to classical compounds, they must have a number of π -electrons equal to $4n + 2$, where $n = 1, 2, 3$, etc. On the other hand, benzenoid compounds are collections of benzene rings with at least one joint side. One of the properties of these classical compounds is that the double bonds do not participate in addition reactions but perform electrophilic substitution reactions, thus preserving the stability of the π -electron system. Except in the case of C-C cleavage at high temperatures or by enzymatic action (Poater et al., 2022). Furthermore, this likely is one of the reasons why the aromatic flavor of the herb fruit is diminished after cooking at high temperatures. L-Cysteine (L-Cys), a non-essential amino acid, was detected in F at a low level of 1.6 %. L-Cys or its esters with aldehydes or ketones react with were obtained the reduced thiazole derivatives.

Two peptides, Lys-Cys and Ala-Gly, were present in this assay and were detected only in D. It has been reported that Lys-Cys is associated with the synthesis of hydrogels and bifunctional supervalent iodine reagents (Chowdhuri et al., 2020, Ceballos et al., 2021). It has been experimentally demonstrated that the mechanism of dipeptide inhibition was simulated using molecular dynamics (MD), and the results showed that the N-terminal end of the dipeptide is the key to the inhibition. Ala-Gly was appraised as an environmentally benign hydrate inhibitors for CH_4 hydrate (Woojin Go et al., 2022). Volatile metabolites are mainly derived from the chemical or enzymatic oxidation of unsaturated fatty acids and from further interactions with proteins, peptides, and free amino acids (Feng et al., 2017).

Inevitably, some pesticides appeared unexpectedly in this study. The source of these pesticides is not the plant's metabolism. During the growth process of grass and fruits, some weeds will appear around the plant, competing for nutrient resources and inhibiting photosynthetic agents for crop weeds. Therefore, growers will use herbicides to inhibit the growth of weeds around the plant and meet the needs of plant growth. And the choice of pesticides needs to comply with the relevant laws and regulations (Institute for the Control of Agrochemicals, 2018).

Esters, with more esters in F, compared to D. The proper level of esters will bring out the fruit flavor. Three were detected in D and eight were detected in F. Most of the naturally occurring fats and oils are fatty acid esters of glycerol. Low molecular weight esters are commonly used as fragrances and are found in essential oils and pheromones, and are more volatile (Sparkman et al., 2011). Esters are polar molecules but have lower boiling points than carboxylic acids and alcohols of similar molecular weight because there are no intermolecular hydrogen bonds between ester molecules. Esters are usually derived from inorganic or organic acids in which at least one hydroxyl group (OH) is replaced by an alkoxy group (-O-alkyl), most often from carboxylic acids and alcohols (Speight, 2011).

The metabolism of amino acids and the oxidation of lipids can decarboxylate to the corresponding aldehydes. Benzaldehyde has an almond and nutty odor and is present in both species. (Verma and Srivastav, 2020) Benzenoid and phenylpropanoid-related volatiles are

derived from the common precursor L-phenylalanine (Verdonk et al., 2003). Benzaldehyde, benzyl alcohol, and benzoic acid are the most common tendencies (Van Moerkercke et al., 2009). A volatile substance, benzaldehyde, exists together in two fruits.

Ketones and phenolic compounds are considered to contribute to the antioxidant potential. Phenols were present in a small percentage of this assay, so it can be determined that phenols do not act as landmarks for D and F. However, phenolics' advantages (HVA) for treating diseases are undeniable. HVA contained in D is a major terminal metabolite of dopamine and one of the three catecholamines produced in the brain. Dopamine is broken down by the liver and excreted as HVA in the urine (Cynthia C. Chernecky PhD, 2013). Also, as a marker of metabolic stress, it is used as a reagent for detecting of oxidative enzymes (Szekely and Didaskalou, 2016). HVA is related to Aromatic L-amino acid decarboxylase deficiency (AADCD) (Manti et al., 2022), Celiac Disease (De Grandis et al., 2010), Breast cancer (Zniber et al., 2022) and Growth-Hormone Deficiency (Zielonka et al., 2015). The 4-Hydroxybenzoic acid detected in F is a phenolic derivative of benzoic acid, which can inhibit most Gram-positive and some Gram-negative bacteria. A study found that p-hydroxybenzoic acid has antiviral activity against SARS-CoV-2. Most promisingly, the study acted on *Candida albicans* by gamma irradiation, which led to the biotransformation of caffeic acid, resulting in a multiplication of its yield (Cho et al., 1998, Singab et al., 2022). Hence, based on the aforementioned results, it can be reaffirmed that D and F exhibit antibacterial effects.

The ketones detected this time contained: 2-Nonanone, 3,4,2,4,6-Pentahydroxychalcone and 2-Undecanone. 2-Undecanone is a volatile organic compound that inhibits DnaKJE-ClpB diketone-dependent refolding of heat-inactivated bacterial fluorophore enzymes. 2-Undecanone can inhibition of tumorigenesis (Melkina et al., 2017, Lou et al., 2019). Flavonoid metabolites in plants are often considered to have neuroprotective, antioxidant, and anticancer properties (Hostetler et al., 2017, Madunic et al., 2018). 3,4,2,4,6-Pentahydroxychalcone belong to the chalcone. Also, relevant chemical elements are classified as minor flavonoids, which play essential roles in plants. It is not a negligible part of their success in adapting to life as sedentary organisms. (Bentrad and Hamida-Ferhat, 2022). D contains ketone compounds, indicating that D is likely to have high medicinal value.

The above study proved that, in general, D contains more types of pharmacologically active substances than F and is relatively rich in them. To a certain extent, this study provides evidence that the pharmacological activity of D is more robust than that of F. It also proved that F has an acidic stimulating sensation regarding taste and flavor.

3.1.3. Discussion: Differential metabolite analysis

A total of 19 differential metabolites were screened, of which 12 were down-regulated and seven were up-regulated (D relative to F, the content of 12 metabolites was higher than that of F, and the content of 7 metabolites was lower than that of F. These differential metabolites are shown in the Table S2. Differential metabolite screening conditions: p -value ≤ 0.05 , VIP ≥ 1 .

In this study, as listed in Table S1, Butyrolactone, 2-Nonanone, Phenol, 3-methyl-, Benzaldehyde, 4-(1-methylethyl)-, *-Muurolene, these types of substances behave up-regulated in D. Bicyclo[3.1.1]heptan-3-ol, 6,6-dimethyl-2-methylene-, [1S-(1*,3*,5*)]- and Cyclohexene, 1-methyl-4-(1-methylethylidene)-, it is up-regulated relative to D. *-Myrcene, 1-Octanol, Naphthalene, decahydro-4a-methyl-1-methylene-7-(1-methylethenyl)-, [4aR-(4a*,7*,8a*)]-, (-)-*-Bourbonene, Butanoic acid, methyl ester, Tetradecane, Pentadecane, Bicyclo [2.2.1]heptan-2-ol, 1,7,7-trimethyl-, acetate, (1S-endo)-, Octanoic acid, methyl ester, (S,1Z,6Z)-8-Isopropyl-1-methyl-5-methylenecyclodeca-1,6-diene, it is obviously only detected in F. Tridecane and Bicyclo[3.1.1]heptane, 6,6-dimethyl-2-methylene-, (1S)-, it exists in the two, and shows a down-regulation to D. Tridecane is a differential metabolite, only exists in D3. All samples of F contain this substance. Tridecane is a component of the plant, playing a role in plant

metabolites and volatile oils. The substance is downregulated.

Butanoic acid, methyl ester is one of the aromas with an apple, banana, and pineapple fragrance in low concentration (Yun-tao Zhang et al., 2009). Tetradecane was also found in mango, which is a recognized fruit aroma substance. And owing to a kind of volatile compounds (Campos Alencar Oldoni et al., 2022). When the thrips felt conspecific extract by the *Liothrips jatrophae*, which include the tridecane, pentadecane, tetradecyl isobutyrate and hexadecyl isobutyrate regards as the major ingredient. That will make thrips show threatened behavior, such as rapid sideways movement and others' reactions (González-Orellana et al., 2021).

Regarding butyrolactone, there is a professional report that γ -butyrolactone and oxazolidinone-based ligands are pharmacologically necessary scaffolds in drug research (Bhandare et al., 2022). Relevant research indicates and proposes key markers for distinguishing the incorporation of quinoa flour into rice and wheat flour, particularly four volatile substances, including butyrolactone, and five other aromatic compounds (Yang et al., 2022). The relevant reached herein that the final heterocycles could be easily transformed γ -butyrolactone attribute to a straightforward photochemical method (Ye et al., 2022).

2-Nonanone is a colorless to light yellow liquid with fruit, flower, oil and herb-like aroma. It is reported that males of *A. mysticus* produce include two component mixture of (R)-3-hydroxy-2-hexanone and 2-nonanone. This pheromone can attract the aggregation of females and males of the same species (Molander et al., 2019).

Phenol,3-methyl-, is also a raw material for highly effective and low toxicity pesticides, such as speedwell and is used in the manufacturing of spices and resins. The presence of the substance is most likely due to the spraying of pesticides by growers during the growth of plants. It is obvious that the pesticide residue was found only in D and at relatively high levels. However, we were unable to determine whether the pesticide residue was enriched in the seed coat or the kernel. If a large amount of D is used, it is one of the breakthrough points that needs to be thoroughly investigated in subsequent studies to determine if it poses a potential health hazard to humans.

Benzaldehyde, 4-(1-methylethyl)- is a natural aldehyde that inhibits α -synuclein fibrillation and cytotoxicity, and has anticancer activity. This metabolite product, we also called Cuminaldehyde. It is direction a particular unit concentration of this substance can inhibit the biofilm formation of *Pseudomonas aeruginosa* and thus act against various acute and chronic infections caused by humans (Chatterjee et al., 2021).

*-Murolene is one of a mixture of six compounds from the pigeon pea plants, which are attracted by steam distillate. It has the phenomenon of attracting female *H. armigera* moths present (Hartlieb and Rembold, 1996). It is known from the literature that this product is also present in the leaves of D (Yong Min et al., 2011). Our team found that there was a severe pest infestation in the area where the grass-fruit plants were planted. Whether this can provide some reference in the subsequent study needs to be studied in depth.

Cyclohexene, 1-methyl-4-(1-methylethylidene)- generated from 15 days of Sichuan sausages (Feng et al., 2017) and essential oils of three peppers (Renjie et al., 2009). Surprisingly, the PubChem database search showed it isomeric with Terpinolene ($C_{10}H_{16}$). However, this metabolite's specific chemical properties and physical qualities still need to be studied more, and it is detected in both D and F.

Myrcene revealed by this detected in the D, not only exists F. However, a researcher detected GC-MS for this chemical component (Yang et al., 2008). Myrcene exists as two isomers: the most natural terpenes were familiar presence occurring β -isomer, and there is less. In cyclization reactions leading to ρ -menthane derived from an isopropylidene group in the naturally isomers. For α -isome that is isopropenyl form, often easily prepared by humans. The chemical is a colorless oil with the characteristic odor of geraniums (Behr and Johnen, 2009). It can be used in perfume industry such as cologne and deodorant, which has a pleasant balsamic scent. Unparalleled importance of 1-octanol for the synthesis of 1-octene, a comonomer for polyethylene (Julis and Leitner,

2012). There is a colorless, transparent, oily liquid with a solid oily odor and citrus scent. Almost insoluble in water but miscible with alcohols, esters, chloroform, etc. Active ingredients from plant volatile compounds can serve as natural gaseous biocides. They regulate the degree of bacterial decay in agricultural products. A professional study revealed that 1-octanol exhibits remarkable antifungal potency, confirming that both the gas and liquid states of 1-octanol are associated with the growth and development of aflatoxin spores under varying exposure concentrations. This leads to irreversible damage to the plasma membrane, resulting in electrolyte leakage (Qin et al., 2022). As to previous research, odor signals could drive honeybee's foraging preferences. (-)- β -bourbonene has reaction as far as bees are concerned. The compound showed a dramatic surge after infection (Antonio Cellini et al., 2018). An investigation with this result suggested the highly probable degradation product of germane-like precursors. A comprehensive experimental in-depth test confirmed that the extract containing bourbonene exhibited a strong anti-tick repellent effect (M. A. Birkett et al., 2008). Recently, a report was bound to investigate the anticancer potential of β -bourbonene on human prostate cancer PC-3 M cells. It was found by biological technology test that the concentration of this substance increased, and the protein expression of Bax was significantly increased in the drug treatment group, while the protein expression of Bcl-2 was decreased. Finally, it was concluded that β -bourbonene could inhibit the proliferation of prostate cancer PC-3 M cells while inducing apoptosis and G0/G1 phase arrest (Wang et al., 2018a; Wang et al., 2018b).

Thereby, 19 differential metabolites were identified according to the screening conditions, as illustrated in Fig. 5. The ordinate refers to the relative quantitative value of the metabolite after normalization. Using the normalized data, the thickest black line in the middle of each box represents the average relative content of this substance in this group. This figure is based on the quantitative value of metabolites and whether the content of metabolites has significant differences between different groups. One asterisk indicates that P is less than 0.05, with a significant difference. The two asterisks are P less than 0.01, with higher significance. If there is no asterisk, there is no significant difference. Note: It should be noted that the 12th tested component is a pesticide, and it is not a result of the plant's metabolites. It can only be used for detecting pesticide residue of exogenous substances.

3.2. Results and discussion of FT-IR analysis

3.2.1. Results: Spectroscopic analysis

Fig. 6 showed the raw averaged NIR spectrum. NIR spectroscopy is a type of high-energy vibrational spectroscopy; Detailed chemical information is displayed in the scope of 750 to 2500 nm (13333 to 4000 cm^{-1}). At the molecular level, the replacement of light atoms (such as hydrogen) by heavy atoms can be sensed by NIR due to its impact on the strength of the remaining bonds and the combination of vibrational modes. The figure illustrates that the peak shapes and positions of the infrared spectra of the two species are identical, while the peak absorbance differs. This suggests that the chemical components of the two species are fundamentally similar, with the difference likely attributable to variations in the accumulation of chemical components. The spectral trends of the two are also comparable. In the original spectrum, the spectral absorbance of F is higher than that of D. Two spectra with similar trends can be clearly seen. It is speculated that this may be related to the selection of samples. The dried fruits from the market are most likely to be stored for a long time. But we can't confirm the storage period, and the research on the storage period of D is also an extremely blank research field for now. FT-NIR can reflect the chemical information of hydrogen-containing organic components (N-H, C-H, O-H) in the samples. The result show that both species have multiple shared peaks at 7000–4000 cm^{-1} and 8500–8000 cm^{-1} . The stretching vibration located between 8380 and 8230 cm^{-1} is the C-H second overtone stretching models in $-CH_3$ (Liu et al., 2021a; Liu et al., 2021b). The first overtone of

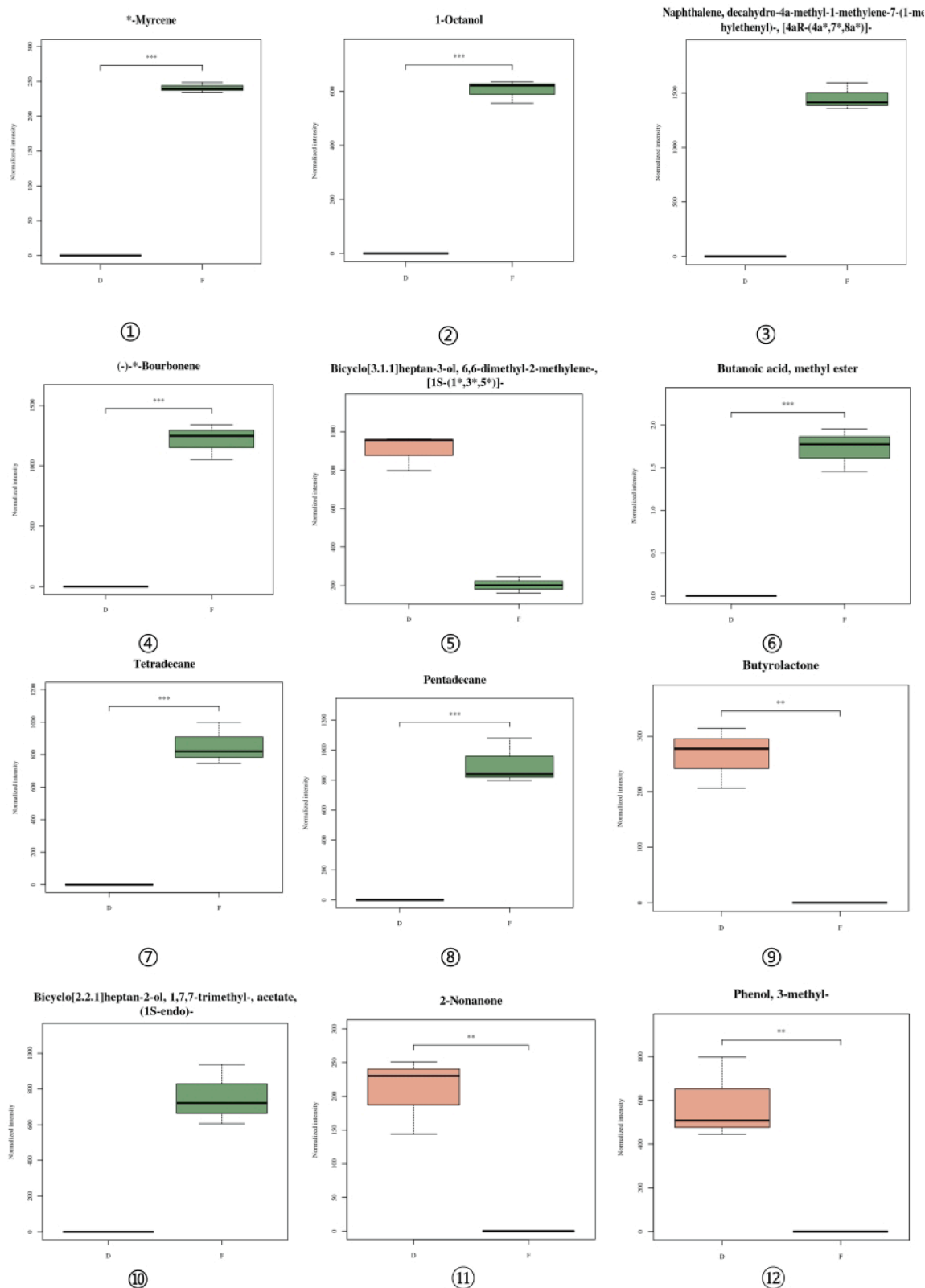


Fig. 5. Box plot of 19 different metabolites of D vs F. (①*-Myrcene; ② 1-Octanol; ③Naphthalene, decahydro-4a-methyl-1-methylene-7-(1-methylethenyl)-, [4aR-(4a*,7*,8a*)]; ④ (-)-*-Bourbonene; ⑤Bicyclo[3.1.1]heptan-3-ol, 6,6-dimethyl-2-methylene-, [1S-(1*,3*,5*)]; ⑥ Butanoic acid, methyl ester; ⑦ Tetradecane; ⑧Pentadecane; ⑨Butyrolactone; ⑩ Bicyclo[2.2.1]heptan-2-ol, 1,7,7-trimethyl-, acetate, (1S-endo)-; ⑪ 2-Nonanone; ⑫ Phenol, 3-methyl-; ⑬ Tridecane; ⑭ Octanoic acid, methyl ester; ⑮ Bicyclo[3.1.1]heptane, 6,6-dimethyl-2-methylene-, (1S)-; ⑯ (S,1Z,6Z)-8-Isopropyl-1-methyl-5-methylenecyclodeca-1,6-diene; ⑰ Benzaldehyde, 4-(1-methylethyl)-; ⑱ *-Muurolene; ⑲ Cyclohexene, 1-methyl-4-(1-methylethylidene)-).

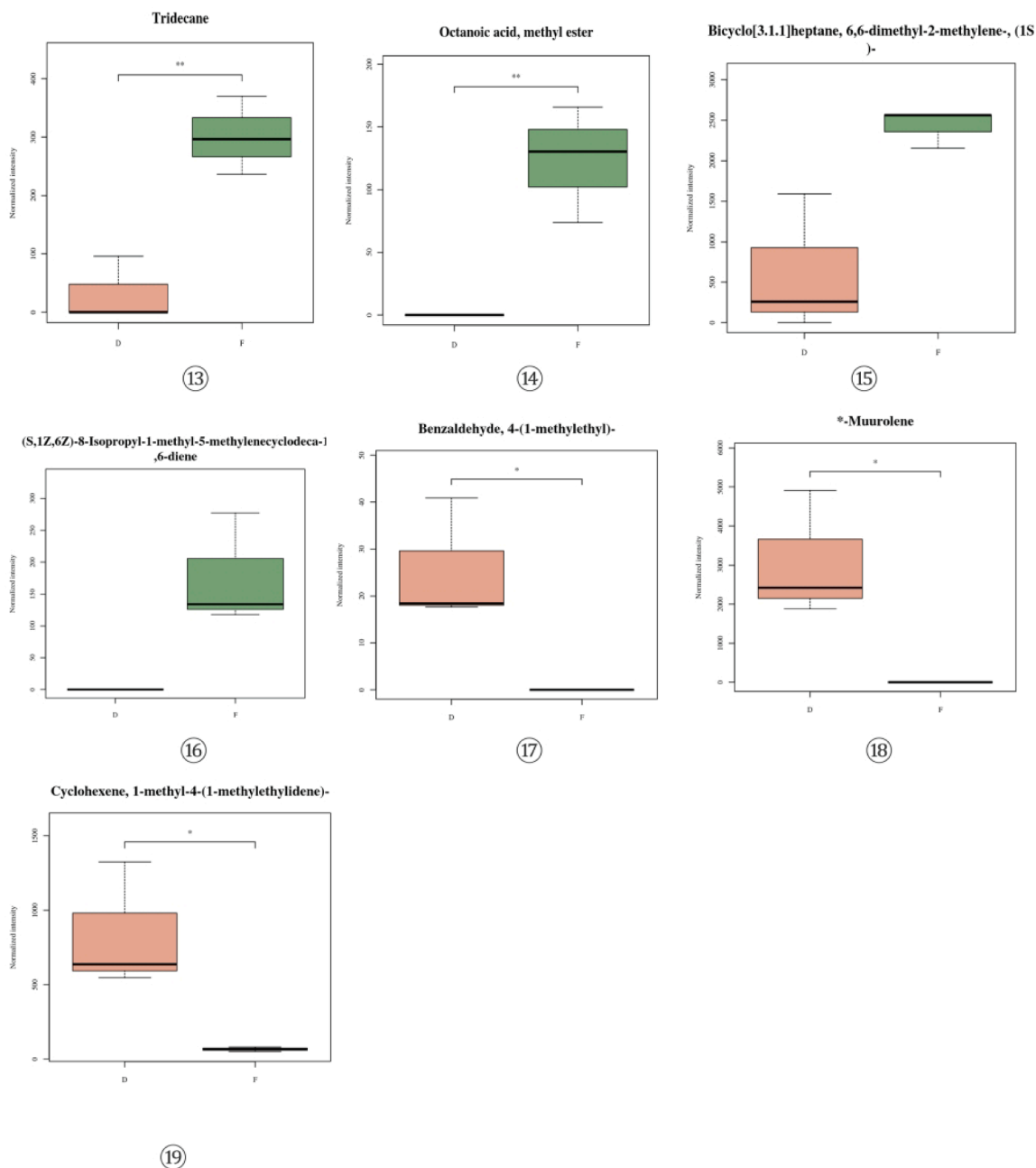


Fig. 5. (continued).

O-H stretching vibrations peaks could be seen near $6900\text{--}6800\text{ cm}^{-1}$. While, the first overtone C-H stretching vibration belonging to $-\text{CH}_2$ could be revealed around $6000\text{--}5400\text{ cm}^{-1}$ (Liu et al., 2021a; Liu et al., 2021b). One of the noticeable points is that around 4400 cm^{-1} , it shown that it is related to the combination band of O-H and C-O stretching modes in glucose, the Table 3 did some summary. Despite specific differences in peak shape, position, and intensity, direct classification and identification of samples from different species through the spectrum is challenging. As a result, the establishment of a classification model with the aid of chemometric methods becomes imperative.

3.2.2. Discussion: Spectral discriminant model effect analysis

As shown in Fig. 7 A, the principal components can explain 96.1 % of the variables after fitting. To verify whether the traditional supervised algorithm PLS-DA can carry out the research exploration of the two species, the construction of a supervised model is therefore proposed.

The results demonstrate a significant classification effect. To investigate the feasibility of employing the traditional supervised algorithm PLS-DA for the research exploration of the two species, we propose the construction of a supervised model.

As a classical linear classification method, it is well-suited for the analysis of intricate and convoluted data matrices. In order to enhance the evaluation of the model's effectiveness, 17 out of 25 samples were chosen as the training set, while the remaining 8 samples were allocated as the test set based on the Kennard-Stone algorithm (KS). And for validating the fitting extent of the final expression, 200-iteration was tested on the permutation test, the effect shown in Figure S4. It can be clearly seen that the value of R^2 is below 0.5, and the value of Q^2 is below 0. This parameter verifies that the model is robust and the fit is in place. The parameters, confusion matrix, and classification results are displayed in Table S4 in the Supplementary Material. It is had to describe that the confusion matrix included the total number of True

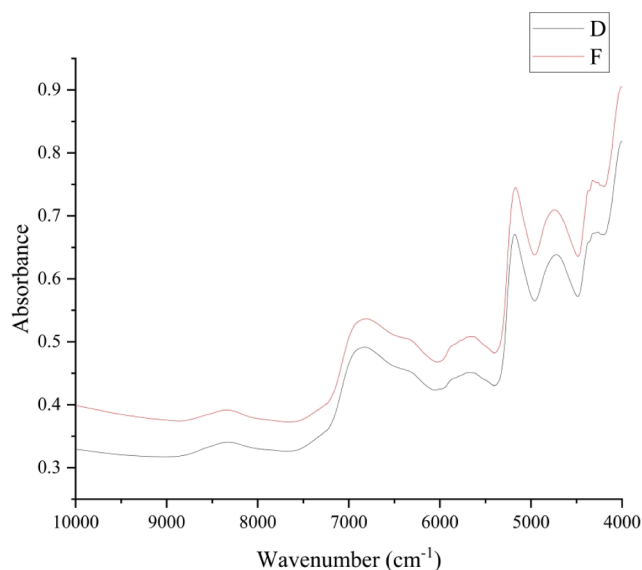


Fig. 6. The Raw of FT-NIR spectrum. D: is the grass fruit, represented by black lines; F: is the nine-foot cardamom, represented by red lines. (For interpretation of the references to color in this figure legend, the reader is referred to the web version of this article.)

Table 3
Peak assignments on the FT-NIR spectra of D and F.

Feature bands (cm ⁻¹)	Wavenumber (cm ⁻¹)	Base group and vibration mode	References
8500–7500	8380	The C-H second overtone stretch vibrations models in -CH ₃	(Liu et al., 2021)
	8230		
6800–6900		Stretch vibration first overtone O-H	
	6953	C-H combination bands in -CH ₂	
	6300	The first overtone -C-H stretching	
	7145	C-H combination bands in -CH ₂	
6000–5400	5180	Polysaccharide combination band of O-H stretching vibration and transformation of H-O-H	
5730–5560		The first overtone -C-H stretching	
	4400	O-H and C-O stretching vibrations combination bands in glucose	
	4295	The first overtone -C-H stretching	

Positive (TP), False Positive (FP), True Negative (TN), and False Negative (FN) of the train and test set of samples. The final confusion matrix resulted that all 17 test samples in the training set were correctly classified with a 100 % classification accuracy value, and the classification results in the test set were also excellent with all 8 samples correctly classified, which shows that the PLS-DA model is robust and accurate for the classification between two species. The parameter display result, the R² is 96.95 %, the Q² is 83.54 %, the result shown in Table 4.

The OPLS-DA is an extension of the PLS algorithm, which naturally simplifies the interpretability of the outcome components and allows additional assessment of intra- and inter-group differences. The unsupervised PCA only indicates the differential nature of the two categories of samples. The final distinction needs to be made with the help of the appropriate supervised methods of PLS. Based on the observation of the replacement test results for 200 iterations, the two PLS models did not show overfitting, which is likely to indicate the feasibility and

robustness of the models. However, the effect of the models after increasing the sample size in this paper is also worth further testing in future studies. The OPLS-DA model has an R² of 96.59 % and a Q² of 86.58 %, with 100 % accuracy values for both the training and prediction sets, indicating the superiority of the model effect.

Finally, the classification effect of the PCA model has reached 96.1 %, the model effect of both PLS-DA and OPLS-DA has reached 100 %, and the prediction performance of the model of OPLS-DA is better than that of PLS-DA from the Q² value. In this study, the data pre-processing phase was omitted due to the high-performance parameters exhibited by the raw data.

4. Discussion

The detected metabolites in comparison to the previous research results consist of terpenes, aldehydes, organic heterocyclic compounds, alcohols, aromatic compounds, esters, ketones, and peptides (Qin et al., 2021). Currently, the increased economic value of the herbaceous fruit has turned it into a cash crop. In contrast, due to its limited cultivation range, the economic value of *A. maximum* has not been fully realized, and its potential uses require further development. Therefore, considering the advantages of *A. maximum* in terms of its use as a spice for removing odors, medicinal treatment for gastrointestinal diseases, and as a fresh fruit, it is urgent to research whether it has a better resource utilization value. This will provide a scientific theoretical basis for promoting *A. maximum* as the next economically important cardamom crop. However, the conditions for GC-MS to detect metabolites are different, and the different metabolites detected are also different, which will bring difficulties to the analysis of the final and accurate results. Therefore, the current metabolomics of *A. tsaoko* and *A. maximum* are only based on the identifying of simple metabolites. On this basis, it is necessary and meaningful to carry out an in-depth exploration of the metabolites of these two species. In the later stage, it is necessary to explore the metabolic mechanism and transparently understand the fruit components of these two species. At present, there has been relatively cutting-edge research on *A. tsaoko*. It assembled the chromosomal level genome of *A. tsaoko*, revealing the content, regulatory genes and synthetic pathway of the special aroma and spicy substances in *A. tsaoko* at different tissue parts and at different ripening stages of the fruit. A single metabolomics technology cannot establish a complete description of plant metabolic pathways or metabolites. In the future, from samples to detection instruments and programs, such as a comparison of fresh fruits and dried fruits, and the direct extraction of essential oil from *A. maximum* for final detection, the compensation of these parts will be a trend of more research significance in the future.

5. Conclusions

This study utilized two modern techniques, SPME-GC-MS and NIR, to classify the dry fruits, *A. tsaoko* and *A. maximum*. Five data analysis methods, including PCA, HCA, PLS-DA, OPLS-DA, and Veen, were employed to analyze the GC-MS data. In the end, a total of 67 kinds of metabolites were detected in *A. tsaoko* and 65 in *A. maximum*. According to the GC-MS metabolic results, a total of 101 substances were detected, 66 products were detected by D, and 64 substances were detected by F, of which 29 were the same substances and 18 were different metabolites. According to the test results, the main categories of metabolites in D have terpenes and alcohols; The main categories in F are terpenes and aldehydes. The classification categories of other products are also very similar, and the number of products tested is inconsistent, which may also be the reason for the difference between the two species. The two species exhibit a total of eight primary categories of metabolites, among which terpenes, aldehydes, and alcohols show notable similarities. The predominant metabolite classes in the final results are terpenes (37.9 %), aldehydes (12.1 %), organic heterocyclic compounds (7.6 %), alcohols (6.1 %), aromatic compounds (4.5 %), esters (4.5 %), ketones (4.5 %),

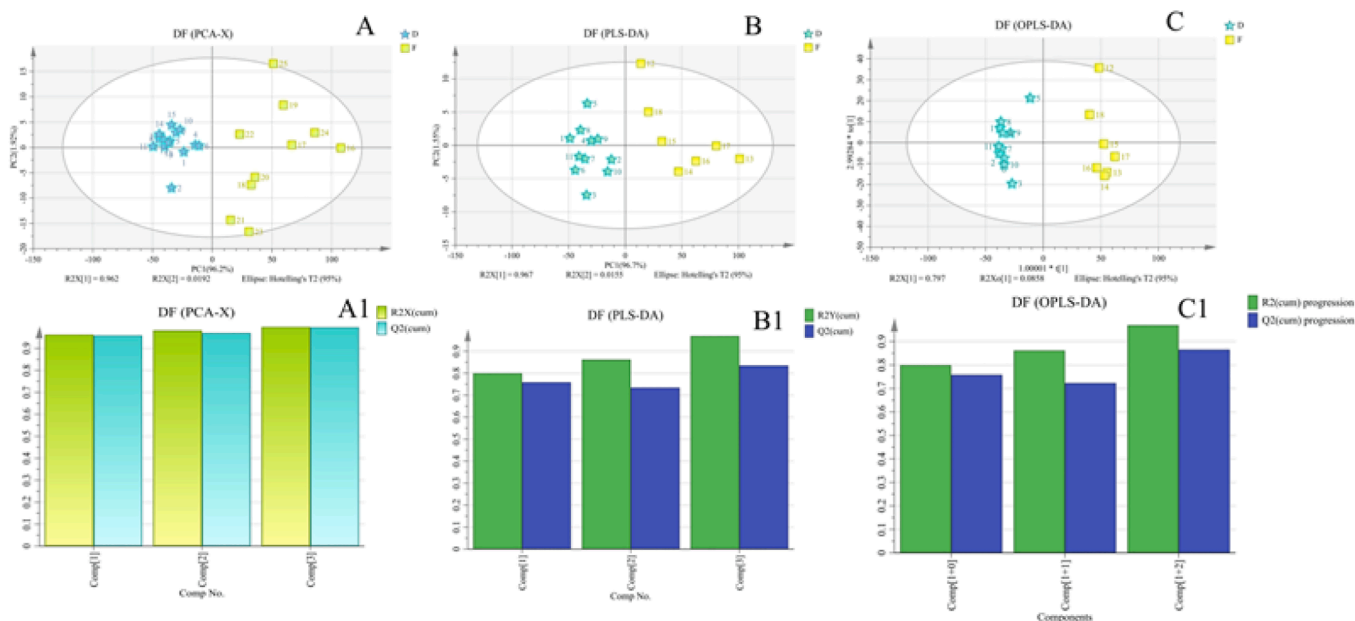


Fig. 7. The FT-IR of visualization model. A: PCA result; B: PLS-DA model; C: OPLS-DA model.

Table 4

Parameters of the sample of the FT-NIR information. Classification results of PCA, PLS-DA and OPLS-DA model.

Model	R ² (%)	Q ² (%)	RMSEE	RMSEcv	RMSEP	ACC Train (%)	ACC Test (%)	LVs
PCA	99.74 %	99.57 %	–	–	–	–	–	3
PLS-DA	96.95 %	83.54 %	0.0965499	0.204674	0.076772	100 %	100 %	3
OPLS-DA	96.95 %	86.58 %	0.0965498	0.178587	0.07677	100 %	100 %	1 + 2 + 1

and peptides (3 %). On the contrary, F is divided into a total of 17 categories, with the main metabolic categories being terpenes (37.5 %), esters (12.5 %), alcohols (9.4 %), aldehydes (6.3 %), alkanes (7.8 %), aromatic compounds (3.1 %), carboxylic acids (3.1 %), and olefins (3.1 %). This could also be attributed to the potential similarity in their therapeutic effects.

From this, it is evident that GC–MS entails cumbersome sample preparation, longer detection times, and higher costs. In the pursuit of rapid and efficient classification, there is still a need to rely on the convenient NIR. The results confirm that relying solely on collected raw spectra is insufficient to achieve clear classification outcomes. The NIR data were subjected to PCA, PLS-DA, and OPLS-DA, three of which demonstrated excellent model performance. Once the NIR data is collected, it requires appropriate data processing methods to compare with the infrared spectra in the database, enabling the accurate and rapid generation of basic classification reports. This study also confirmed this. In conclusion, both detection techniques are capable of classifying two species, and the data model performance is good. Compared to the metabolite results from GC–MS detection, infrared spectroscopy offers a more direct and rapid detection method.

Author Contributions

Fengjiao Li: Conceptualization, Data curation, Writing – original draft, Writing – review & editing, Visualization, Investigation, Validation, Formal analysis, Methodology, Software; Weize Yang: Investigation, Supervision, Resources; Meiquan Yang: Investigation, Supervision, Resources; Yuanzhong Wang and Jinyu Zhang: Conceptualization, Funding acquisition, Writing – original draft, Writing – review & editing, Validation, Supervision, Project administration, Software.

Funding

This research was funded by: 1. Rural Revitalization Science and Technology Special Project, Science and Technology Delegation of Dulongjiang Township, Gongshan County, Yunnan Province; Grant Number: 202304BI090032-17; 2. Yunnan Province's major science and technology special plan project "Nujiang Grass and Fruit Industry Science and Technology Innovation and Application Research", Grant Number: 202202AE090035; 3. Yunnan Provincial Innovation Guidance and Scientific and Technological Enterprise Cultivation Plan "Yunnan Fugong Grass Fruit Industry Science and Technology Mission", Grant Number: 202104BI090011.

CRediT authorship contribution statement

Fengjiao Li: Conceptualization, Data curation, Writing – original draft, Writing – review & editing, Visualization, Investigation, Validation, Formal analysis, Methodology, Software. **Weize Yang:** Investigation, Supervision, Resources. **Meiquan Yang:** Investigation, Supervision, Resources. **Yuanzhong Wang:** Conceptualization, Funding acquisition, Writing – original draft, Writing – review & editing, Validation, Supervision, Project administration, Software. **Jinyu Zhang:** Conceptualization, Funding acquisition, Writing – original draft, Writing – review & editing, Validation, Supervision, Project administration, Software.

Declaration of Competing Interest

The authors declare that they have no known competing financial interests or personal relationships that could have appeared to influence the work reported in this paper.

Appendix A. Supplementary data

The following supporting information can be downloaded at: www.mdpi.com, Figure S1 The HCA about D vs F; Figure S2 Veen diagram of *Amomum tsaoko* Crevost et Lemarie (D) and *Amomum maximum* Roxb. (F); Figure S3 Relative content histogram of D and F.; Figure S4 PLS-DA: 200-iteration was tested on the permutation test. Figure S5 The D of the chemical composition (difference section, The more details in the Table S5); Figure S6 The F of the chemical composition (difference section, The more details in the Table S5); Figure S7 D vs F of the same chemical composition. (The more details in the Table S5). Supplementary data to this article can be found online at <https://doi.org/10.1016/j.arabjc.2024.105665>.

References

- Arthur, C.L., Pawliszyn, J., 1990. Solid phase microextraction with thermal desorption using fused silica optical fibers. *Anal. Chem.* 62, 2145–2148. <https://doi.org/10.1021/ac00218a019>.
- Behr, A., Johnen, L., 2009. Myrcene as a natural base chemical in sustainable chemistry: a critical review. *ChemSusChem* 2, 1072–1095. <https://doi.org/10.1002/cssc.200900186>.
- Bentrad, N. and A. Hamida-Ferhat, 2022. Chapter 3 - Analytical approaches used in the profiling of natural products with a therapeutic target: a global perspective on nutrition and health. *Studies in Natural Products Chemistry*. R. Atta ur, Elsevier. 72: 57–101.
- Bhandare, R.R., Sigalappali, D.K., Shaik, A.B., et al., 2022. Selectivity profile comparison for certain γ -butyrolactone and oxazolindione-based ligands on a sigma 2 receptor over sigma 1: a molecular docking approach. *RSC Adv.* 12, 20096–20109. <https://doi.org/10.1039/d2ra03497b>.
- Birkett, M.A., Abassi, S.A., Krober, T., et al., 2008. Antiectoparasitic activity of the gum resin, gum haggard, from the East African plant, *Commiphora holtziana*. *Phytochemistry* 69, 1710–1715. <https://doi.org/10.1016/j.phytochem.2008.02.017>.
- Boysen, R. I. and M. T. W. Hearn, 2010. 7.14 - High Performance Liquid Chromatographic Separation Methods. *Comprehensive Natural Products III*. H.-W. Liu and T. P. Begley. Oxford, Elsevier: 280–311.
- Ceballos, J., Grinhagena, E., Sangouard, G., et al., 2021. Cys-Cys and Cys-Lys Stapling of Unprotected Peptides Enabled by Hypervalent Iodine Reagents. *Angew. Chem. Int. Ed.* 60, 9022–9031. <https://doi.org/10.1002/anie.202014511>.
- Cellini, A., Giacomuzzi, V., Donati, L., et al., 2018. Pathogen-induced changes in floral scent may increase honeybee-mediated dispersal of *Erwinia amylovora*. *ISME J.* 13, 847–859. <https://doi.org/10.1038/s41396-018-0319-2>.
- Chatterjee, S., Paul, P., Chakraborty, P., et al., 2021. Cuminaldehyde exhibits potential antibiofilm activity against *Pseudomonas aeruginosa* involving reactive oxygen species (ROS) accumulation: a way forward towards sustainable biofilm management. *3 Biotech* 11, 485. <https://doi.org/10.1007/s13205-021-03013-1>.
- Chetia, M., Giri, B.R., Swargiary, A., et al., 2014. *Amomum maximum* Roxb (Zingiberaceae), a Medicinal Plant of Tripura, India: A Natural Anthelmintic? *J. Adv. Microsc. Res.* 9, 148–153. <https://doi.org/10.1166/jamr.2014.1206>.
- Cho, J.-Y., Moon, J.H., Seong, K.Y., et al., 1998. Antimicrobial activity of 4-hydroxybenzoic acid and *trans* 4-hydroxycinnamic acid isolated and identified from rice hull. *Biosci. Biotech. Biochem.* 62, 2273–2276. <https://doi.org/10.1271/bbb.62.2273>.
- Chowdhuri, S., Saha, A., Pramanik, B., et al., 2020. Smart thixotropic hydrogels by Disulfide-Linked short peptides for effective Three-Dimensional cell proliferation. *Langmuir* 36, 15450–15462. <https://doi.org/10.1021/acs.langmuir.0c03324>.
- Cui, Q., Wang, L.T., Liu, J.Z., et al., 2017. Rapid extraction of *Amomum tsaoko* essential oil and determination of its chemical composition, antioxidant and antimicrobial activities. *J. Chromatogr. B* 1061–1062, 364–371. <https://doi.org/10.1016/j.jchromb.2017.08.001>.
- Cynthia C. Chernecky PhD, R., CNS, AOCN, FAAN, Barbara J. Berger MSN, RN, CNS, 2013. *H. Laboratory Tests and Diagnostic Procedures* 602–667.
- De Grandis, E., Serrano, M., Perez-Duenas, B., et al., 2010. Cerebrospinal fluid alterations of the serotonin product, 5-hydroxyindolacetic acid, in neurological disorders. *J. Inherit. Metab. Dis.* 33, 803–809. <https://doi.org/10.1007/s10545-010-9200-9>.
- Fan, H., Chen, M., Dai, T., et al., 2023. Phenolic compounds profile of *Amomum tsaoko* Crevost et Lemaire and their antioxidant and hypoglycemic potential. *Food Biosci.* 52. <https://doi.org/10.1016/j.fbio.2023.102508>.
- Feng, C.-H., Liu, Y.-W., Makino, Y., et al., 2017. Evaluation of modified casings and chitosan-PVA packaging on the physicochemical properties of cooked Sichuan sausages during long-term storage. *Int. J. Food Sci. Technol.* 52, 1777–1788. <https://doi.org/10.1111/ijfs.13451>.
- Frank, L., Wenig, M., Ghirardo, A., et al., 2021. Isoprene and beta-caryophyllene confer plant resistance via different plant internal signalling pathways. *Plant, Cell Environ.* 44, 1151–1164. <https://doi.org/10.1111/pce.14010>.
- Go, W., Yun, S., Lee, D., et al., 2022. Dipeptides as environmentally friendly CH₄ hydrate inhibitors: experimental and computational approaches. *Fuel* 329, 125479. <https://doi.org/10.1016/j.fuel.2022.125479>.
- González-Orellana, J., López-Guillén, G., Malo, E.A., et al., 2021. Behavioural and electrophysiological responses of *Liothrips jatrophae* (Thysanoptera: Phlaeothripidae) to conspecific extracts and some of its identified compounds. *Physiol. Entomol.* 47, 11–19. <https://doi.org/10.1111/phen.12367>.
- Goyal, S., Lambert, C., Cluzet, S., et al., 2012. Secondary metabolites and plant defence. In: Méridon, J.M., Ramawat, K.G. (Eds.), *Plant Defence: Biological Control*. Dordrecht, Springer, Netherlands, pp. 109–138.
- Guo, S.-S., You, C.-X., Liang, J.-Y., et al., 2015. Essential Oil of *Amomum maximum* Roxb. and Its Bioactivities against Two Stored-Product Insects. *J. Oleo Sci.* 64, 1307–1314. <https://doi.org/10.5650/jos.ess15160>.
- Guo, N.a., Zang, Y.-P., Cui, Q.i., et al., 2017. The preservative potential of *Amomum tsaoko* essential oil against *E. coli*, its antibacterial property and mode of action. *Food Control* 75, 236–245. <https://doi.org/10.1016/j.foodcont.2016.12.013>.
- Haleva-Toledo, E., Naim, M., Zehavi, U., et al., 1999. Formation of α -terpineol in citrus juices, model and buffer solutions. *J. Food Sci.* 64, 838–841.
- Hartlieb, E., Rembold, H., 1996. Behavioral response of female *Helicoverpa (Heliolithis) armigera* HB. (Lepidoptera: Noctuidae) moths to synthetic pigeonpea (Cajanus cajan L.) kairomone. *J. Chem. Ecol.* 22, 821–837. <https://doi.org/10.1007/bf02033589>.
- Haspel, J.A., Chetimada, S., Shaik, R.S., et al., 2014. Circadian rhythm reprogramming during lung inflammation. *Nat. Commun.* 5, 4753. <https://doi.org/10.1038/ncomms5753>.
- He, X.F., Zhang, X.K., Geng, C.A., et al., 2020. Tsaokopyranols A-M, 2,6-epoxydiarylheptanoids from *Amomum tsaoko* and their alpha-glucosidase inhibitory activity. *Bioorg. Chem.* 96, 103638. <https://doi.org/10.1016/j.bioorg.2020.103638>.
- Hew, P.S., Selamat, J., Jambari, N.N., et al., 2024. Quality and Safety of Food Product – Current Assessment, Issues, and Metabolomics As A Way Forward. *Food Chemistry Advances*. <https://doi.org/10.1016/j.focha.2024.100632>.
- Hostetler, G.L., Ralston, R.A., Schwartz, S.J., 2017. Flavones: food sources, bioavailability, metabolism, and bioactivity. *Adv. Nutr.* 8, 423–435. <https://doi.org/10.3945/an.116.012948>.
- Huang, J., 2017. A Wild Plant with Great Development Potential - *Amomum maximum* Roxb. Retrieved 2017–10-31, from. https://www.xtbg.ac.cn/xwzx/ylxx/201710/t20171031_4881756.html.
- Huang, M., Abel, C., Sohrabi, R., et al., 2010. Variation of herbivore-induced volatile terpenes among Arabidopsis ecotypes depends on allelic differences and subcellular targeting of two terpene synthases, TPS02 and TPS03. *Plant Physiol.* 153, 1293–1310. <https://doi.org/10.1104/pp.110.154864>.
- Huiwei, Q., Yuanzhong, W., Meiqian, Y., et al., 2021. Medicinal Textual Research of Tsaoko Fructus. *Chin. J. Exp. Tradit. Med. Formulae* 139–148. <https://doi.org/10.13422/j.cnki.syfxj.20210216>.
- Institute for the Control of Agrochemicals, C., 2018. Guideline for safety application of pesticides(X), General Administration of Quality Supervision, Inspection and Quarantine of the People's Republic of China; Standardization Administration of the People's Republic of China. GB/T 8321.10-2018: 72.
- Ji, K.-L., Fan, Y.-Y., Ge, Z.-P., et al., 2018. Maximumins A-D, Rearranged Labdane-Type Diterpenoids with Four Different Carbon Skeletons from *Amomum maximum*. *J. Org. Chem.* 84, 282–288. <https://doi.org/10.1021/acs.joc.8b02665>.
- JR., R. H. H., Z. J. R. B.S., R. D. K. M.D., et al., 1981. Tetrachloroazobenzene in 3,4-dichloroaniline and its herbicidal derivatives: propanil, diuron, linuron, and neburon. *Archives of Environmental Health: Int. J.* 36, 11–14. Doi: 10.1080/00039896.1981.10667599.
- Julis, J., Leitner, W., 2012. Synthesis of 1-octanol and 1,1-dioctyl ether from biomass-derived plant chemicals. *Angew. Chem. Int. Ed.* 51, 8615–8619. <https://doi.org/10.1002/anie.201203669>.
- Karlsson Green, K., 2021. The effects of host plant species and larval density on immune function in the polyphagous moth *Spodoptera littoralis*. *Ecol. Evol.* 11, 10090–10097. <https://doi.org/10.1002/ece3.7802>.
- Kieffer, D.A., Piccolo, B.D., Vaziri, N.D., et al., 2016. Resistant starch alters gut microbiome and metabolic profiles concurrent with amelioration of chronic kidney disease in rats. *Am. J. Physiol.-Renal Physiol.* 310, F857–F871. <https://doi.org/10.1152/ajprenal.00513.2015>.
- Koyama, S., Purk, A., Kaur, M., et al., 2019. Beta-caryophyllene enhances wound healing through multiple routes. *PLoS One* 14, e0216104.
- Kuang, L., Li, C., Cao, S., et al., 2020. *Pharmacopoeia of the People's Republic of China. Medical Science and Technology Press, China.*
- Leather, S. R., 2009. Host-plant selection by phytophagous insects. By E.A. Bernays and R.F. Chapman. (London: Chapman and Hall, 1994). xiii+312 pp. Soft cover £55.00. ISBN 0-412-03131-0 (sc); 0-412-03111-6 (hc). *Bullet. Entomol. Res.* 84, 591–592. 10.1017/s0007485300032855.
- Li, P., Bai, G., He, J., et al., 2022. Chromosome-level genome assembly of *Amomum tsaoko* provides insights into the biosynthesis of flavor compounds. *Hortic. Res.* <https://doi.org/10.1093/hr/uhac211>.
- Liang, M., Zhang, Z., Wu, Y., et al., 2023. Comparison of *Amomum tsaoko* crevost et Lemaire from four regions via headspace solid-phase microextraction: Variable optimization and volatile characterization. *Ind. Crop. Prod.* 191. <https://doi.org/10.1016/j.indcrop.2022.115924>.
- Lim, T.K., 2013. *Amomum tsaoko*. *Edible Med. Non-Medic. Plants* 813–817.
- Lin, Y.i., Huang, M., Guiping, W.u., et al., 2022. Different Methods for Extracting Oleoresin from *Amomum Tsaoko* and Its Composition Analysis. *Modern Food Sci Technol.* 38, 206–217. <https://doi.org/10.13982/j.mfst.1673-9078.2022.2.0524>.
- Liu, H., Yan, Q., Zou, D., et al., 2018. Identification and bioactivity evaluation of ingredients from the fruits of *Amomum tsaoko* Crevost et Lemaire. *Phytochem. Lett.* 28, 111–115. <https://doi.org/10.1016/j.phytol.2018.10.007>.
- Liu, Z., Yang, S., Wang, Y., et al., 2021a. Discrimination of the fruits of *Amomum tsaoko* according to geographical origin by 2DCOS image with RGB and Resnet image analysis techniques. *Microchem. J.* 169, 106545. <https://doi.org/10.1016/j.microc.2021.106545>.

- Liu, Z., Yang, S., Wang, Y., et al., 2021b. Multi-platform integration based on NIR and UV-Vis spectroscopies for the geographical traceability of the fruits of *Amomum tsao-ko*. *Spectrochim. Acta A Mol. Biomol. Spectrosc.* 258, 119872 <https://doi.org/10.1016/j.saa.2021.119872>.
- Lou, Y., Guo, Z., Zhu, Y., et al., 2019. Houttuynia cordata Thunb. and its bioactive compound 2-undecanone significantly suppress benzo(a)pyrene-induced lung tumorigenesis by activating the Nrf2-HO-1/NQO-1 signaling pathway. *J. Exp. Clin. Cancer Res.* 38, 242. <https://doi.org/10.1186/s13046-019-1255-3>.
- Lu, C.-L., Wang, L.-N., Li, Y.-J., et al., 2021. Anti-hyperglycaemic effect of labdane diterpenes isolated from the rhizome of *Amomum maximum* Roxb., an edible plant in Southwest China. *Nat. Prod. Res.* 36, 2570–2574. <https://doi.org/10.1080/14786419.2021.1903006>.
- Luo, J.-G., Yin, H., Fan, B.-Y., et al., 2014. Labdane Diterpenoids from the Roots of *Amomum maximum* and Their Cytotoxic Evaluation. *Helv. Chim. Acta* 97, 1140–1145.
- Madunic, J., Madunic, I.V., Gajski, G., et al., 2018. Apigenin: a dietary flavonoid with diverse anticancer properties. *Cancer Lett.* 413, 11–22. <https://doi.org/10.1016/j.canlet.2017.10.041>.
- Manti, F., Mastrangelo, M., Battini, R., et al., 2022. Long-term neurological and psychiatric outcomes in patients with aromatic L-amino acid decarboxylase deficiency. *Parkinsonism Relat. Disord.* 103, 105–111. <https://doi.org/10.1016/j.parkreldis.2022.08.033>.
- Melkina, O.E., Khmel, I.A., Plyuta, V.A., et al., 2017. Ketones 2-heptanone, 2-nonanone, and 2-undecanone inhibit DnaK-dependent refolding of heat-inactivated bacterial luciferases in *Escherichia coli* cells lacking small chaperon IbpB. *Appl. Microbiol. Biotechnol.* 101, 5765–5771. <https://doi.org/10.1007/s00253-017-8350-1>.
- Min, Y., Zhang, W., Yao, L., et al., 2011. Study on the Essential Oil Chemical Ingredients of *A. tsao-ko* Crevost et Lemaire from Different Regions of Yunnan Province. *Journal of Anhui. Agric. Sci.* 39, 3298–3300. <https://doi.org/10.13989/j.cnki.0517-6611.2011.06.077>.
- Molander, M.A., Eriksson, B., Winde, I.B., et al., 2019. The aggregation-sex pheromones of the cerambycid beetles *Anaglyptus mysticus* and *Xylotrechus antilope* ssp. antilope: new model species for insect conservation through pheromone-based monitoring. *Chemoecology* 29, 111–124. <https://doi.org/10.1007/s00049-019-00281-5>.
- Oldoni, C.A., Florencio, F.C., Brait Bertazzo, G., et al., 2022. Fruit quality parameters and volatile compounds from 'Palmer' mangoes with internal breakdown. *Food Chem.* 388, 132902 <https://doi.org/10.1016/j.foodchem.2022.132902>.
- Poater, J., Vinas, C., Ollid, D., et al., 2022. Aromaticity and Extrusion of Benzenoids Linked to [α-COSAN](-): Clar Has the Answer. *Angew. Chem. Int. Ed.* 61, e202200672.
- Qin, H., Wang, Y., Yang, W., et al., 2021. Comparison of metabolites and variety authentication of *Amomum tsao-ko* and *Amomum paratsao-ko* using GC-MS and NIR spectroscopy. *Sci. Rep.* 11, 15200. <https://doi.org/10.1038/s41598-021-94741-0>.
- Qin, Y.L., Zhang, S.B., Lv, Y.Y., et al., 2022. The antifungal mechanisms of plant volatile compound 1-octanol against *Aspergillus flavus* growth. *Appl. Microbiol. Biotechnol.* 106, 5179–5196. <https://doi.org/10.1007/s00253-022-12049-z>.
- Renjite, L., Shidi, S., Yongjun, M., 2009. Analysis of volatile oil composition of the peppers from different production areas. *Med. Chem. Res.* 19, 157–165. <https://doi.org/10.1007/s00044-009-9180-1>.
- Sabalal, N., Baby, S., 2021. Chemistry of *Amomum* essential oils. *J. Essent. Oil Res.* 33, 427–441. <https://doi.org/10.1080/10412905.2021.1899065>.
- Shi, S., Luo, Y., Ma, Y., et al., 2021. Identification of in vitro-in vivo components of Caoguo using accelerated solvent extraction combined with gas chromatography-mass spectrometry integrated with network pharmacology on indigestion. *Ann. Translat. Med.* 9, 1247. <https://doi.org/10.21037/atm-21-3245>.
- Singab, R.A., Elleboudy, N.S., Elkhatib, W.F., et al., 2022. Improvement of caffeic acid biotransformation into para-hydroxybenzoic acid by *Candida albicans* CI-24 via gamma irradiation and model-based optimization. *Biotechnol. Appl. Biochem.* 69, 469–478. <https://doi.org/10.1002/bab.2124>.
- Sparkman, O.D., Penton, Z.E., Kitson, F.G., 2011. Chapter 15 - Esters. In: Sparkman, O.D., Penton, Z.E., Kitson, F.G. (Eds.), *Gas Chromatography and Mass Spectrometry* (second Edition). Academic Press, Amsterdam, pp. 285–292.
- Speight, J.G., 2011. Chapter 1 - Chemistry and Chemical Technology. In: Speight, J.G. (Ed.), *Handbook of Industrial Hydrocarbon Processes*. Gulf Professional Publishing, Boston, pp. 1–41.
- Starkenmann, C., Mayenzet, F., Brauchli, R., et al., 2007. Structure Elucidation of a Pungent Compound in Black Cardamom: *Amomum tsao-ko* Crevost et Lemarié (Zingiberaceae). *J. Agric. Food Chem.* 55, 10902–10907. <https://doi.org/10.1021/jf072707b>.
- Szekely, G., Didaskalou, C., 2016. Biomimics of Metalloenzymes via Imprinting. *Molecul. Imprinted Catal.* 121–158.
- Trygg, J., Wold, S., 2002. Orthogonal projections to latent structures (O-PLS). *J. Chemom.* 16, 119–128. <https://doi.org/10.1002/cem.695>.
- Van Moerkercke, A., Schauvinhold, I., Pichersky, E., et al., 2009. A plant thiolase involved in benzoic acid biosynthesis and volatile benzenoid production. *Plant J.* 60, 292–302. <https://doi.org/10.1111/j.1365-313X.2009.03953.x>.
- Verdonk, J.C., Ric de Vos, C.H., Verhoeven, H.A., et al., 2003. Regulation of floral scent production in petunia revealed by targeted metabolomics. *Phytochemistry* 62, 997–1008. [https://doi.org/10.1016/s0031-9422\(02\)00707-0](https://doi.org/10.1016/s0031-9422(02)00707-0).
- Verma, D.K., Srivastav, P.P., 2020. A paradigm of volatile aroma compounds in rice and their product with extraction and identification methods: a comprehensive review. *Food Res. Int.* 130, 108924 <https://doi.org/10.1016/j.foodres.2019.108924>.
- Wagner, K.H., Elmadfa, I., 2003. Biological relevance of terpenoids: Overview focusing on mono-, di- and tetraterpenes. *Ann. Nutr. Metab.* 47, 95–106. <https://doi.org/10.1159/000070030>.
- Wang, J., Li, Y., Lu, Q., et al., 2021. Drying temperature affects essential oil yield and composition of black cardamom (*Amomum tsao-ko*). *Ind. Crop. Prod.* 168, 113580. <https://doi.org/10.1016/j.indcrop.2021.113580>.
- Wang, Z., Liu, F., Yu, J.J., et al., 2018b. β-Bourbonene attenuates proliferation and induces apoptosis of prostate cancer cells. *Oncol. Lett.* 16, 4519–4525. <https://doi.org/10.3892/ol.2018.9183>.
- Wang, H., Ma, D., Yang, J., et al., 2018a. An integrative volatile terpenoid profiling and transcriptomics analysis for Gene mining and functional characterization of AvBPPS and AvPS involved in the monoterpenoid biosynthesis in *Amomum villosum*. *Front. Plant Sci.* 9, 846. <https://doi.org/10.3389/fpls.2018.00846>.
- Wang, J.B., Pu, S.B., Sun, Y., et al., 2014. Metabolomic profiling of autoimmune hepatitis: the diagnostic utility of nuclear magnetic resonance spectroscopy. *J. Proteome Res.* 13, 3792–3801. <https://doi.org/10.1021/pr500462f>.
- Yang, X., Xing, B., Guo, Y., et al., 2022. Rapid, accurate and simply-operated determination of laboratory-made adulteration of quinoa flour with rice flour and wheat flour by headspace gas chromatography-ion mobility spectrometry. *LWT Food Sci. Technol.* 167, 113814 <https://doi.org/10.1016/j.lwt.2022.113814>.
- Yang, Y., Yan, R.-W., Cai, X.-Q., et al., 2008. Chemical composition and antimicrobial activity of the essential oil of *Amomum tsao-ko*. *J. Sci. Food Agric.* 88, 2111–2116. <https://doi.org/10.1002/jsfa.3321>.
- Yang, Y., Yue, Y., Runwei, Y., et al., 2010. Cytotoxic, apoptotic and antioxidant activity of the essential oil of *Amomum tsao-ko*. *Bioresour. Technol.* 101, 4205–4211. <https://doi.org/10.1016/j.biortech.2009.12.131>.
- Ye, H.B., Zhou, X.Y., Li, L., et al., 2022. Photochemical synthesis of succinic Ester-Containing phenanthridines from Diazo compounds as 1,4-Dicarbonyl precursors. *Org. Lett.* 24, 6018–6023. <https://doi.org/10.1021/acs.orglett.2c02313>.
- Yuan, M., Breitkopf, S.B., Yang, X., et al., 2012. A positive/negative ion-switching, targeted mass spectrometry-based metabolomics platform for bodily fluids, cells, and fresh and fixed tissue. *Nat. Protoc.* 7, 872–881. <https://doi.org/10.1038/nprot.2012.024>.
- Zhang, Y.-T., Wang, G.-X., Dong, J., et al., 2009. Analysis of volatile components in strawberry cultivars Xingdu 1 and Xingdu 2 and their Parents. *Agric. Sci. China* 8, 441–446.
- Zhangguo Lu, Pengjun Wang, Shigematsu Masami, et al., 2010. Study on Aroma Components of *Tasoko Amomum* by HS-SPME and GC-MS. *Favour Fragrance Cosmet.* 17–21.
- Zhou, W., Wieczorek, M.N., Javanmardi, H., et al., 2023. Direct solid-phase microextraction-mass spectrometry facilitates rapid analysis and green analytical chemistry. *TrAC Trends Anal. Chem.* 166 <https://doi.org/10.1016/j.trac.2023.117167>.
- Zielonka, M., Makhseed, N., Blau, N., et al., 2015. Dopamine-Responsive Growth-Hormone deficiency and central hypothyroidism in septipaterin reductase deficiency. *JIMD Reports* 24, 109–113. <https://doi.org/10.1007/8904.2015.450>.
- Zniber, M., Vahdatiyekta, P., Roy, S., et al., 2022. Electrochemical detection of homovanillic acid, a breast cancer biomarker, using Pluronic-modified MoS₂ nanosheets. *Nano Fut.* 6, 035002 <https://doi.org/10.1088/2399-1984/ac8215>.